

Single-photon detectors in micro-electronics technology – part 2

Claudio Piemonte

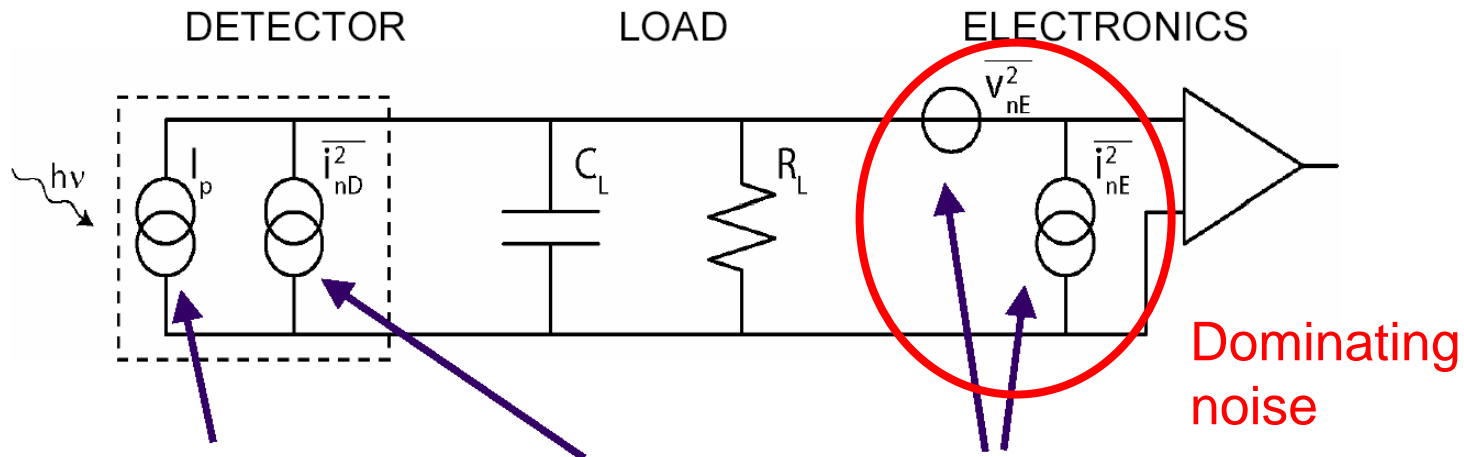
Chief Scientist, Fondazione Bruno Kessler

piemonte@fbk.eu

Low-level light detection technologies

Recap

The problem: **processing of extremely weak signals**



Current signal:
1 pair/photon

Detector noise:
fluctuation of leakage
current

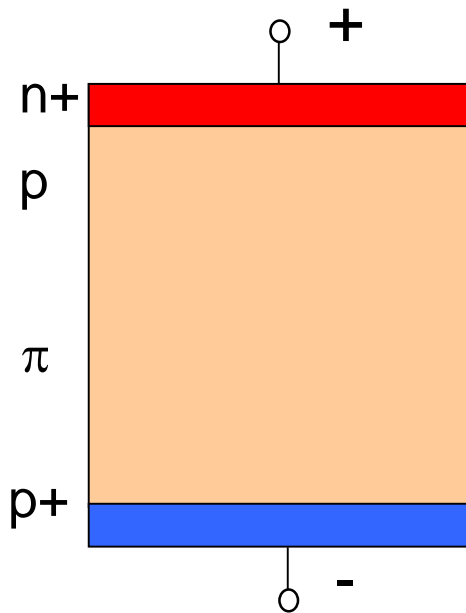
Electronics noise:
shot + thermal noise

**Need of a detector with internal amplification
to reduce the impact of electronic noise!**

Solid-state photodetectors with internal gain.

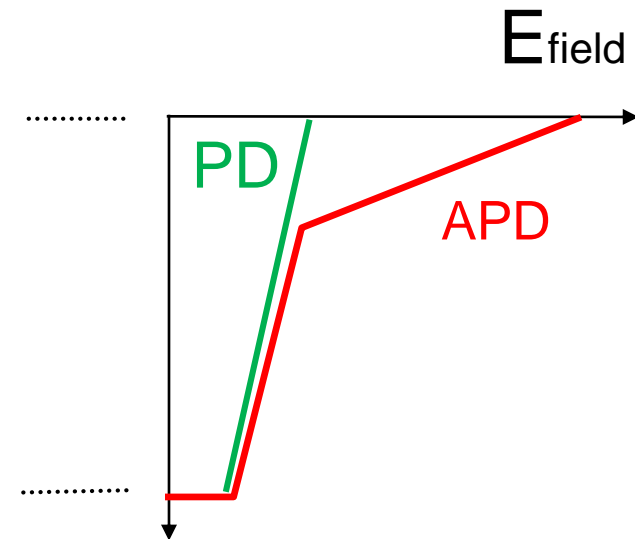
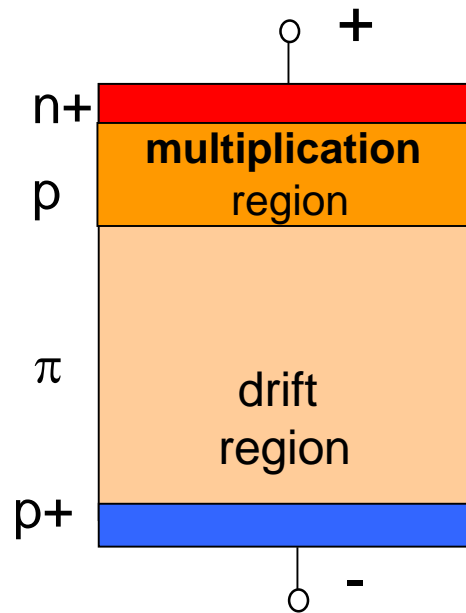
Detectors with gain

Photodiode



1 photo-carrier

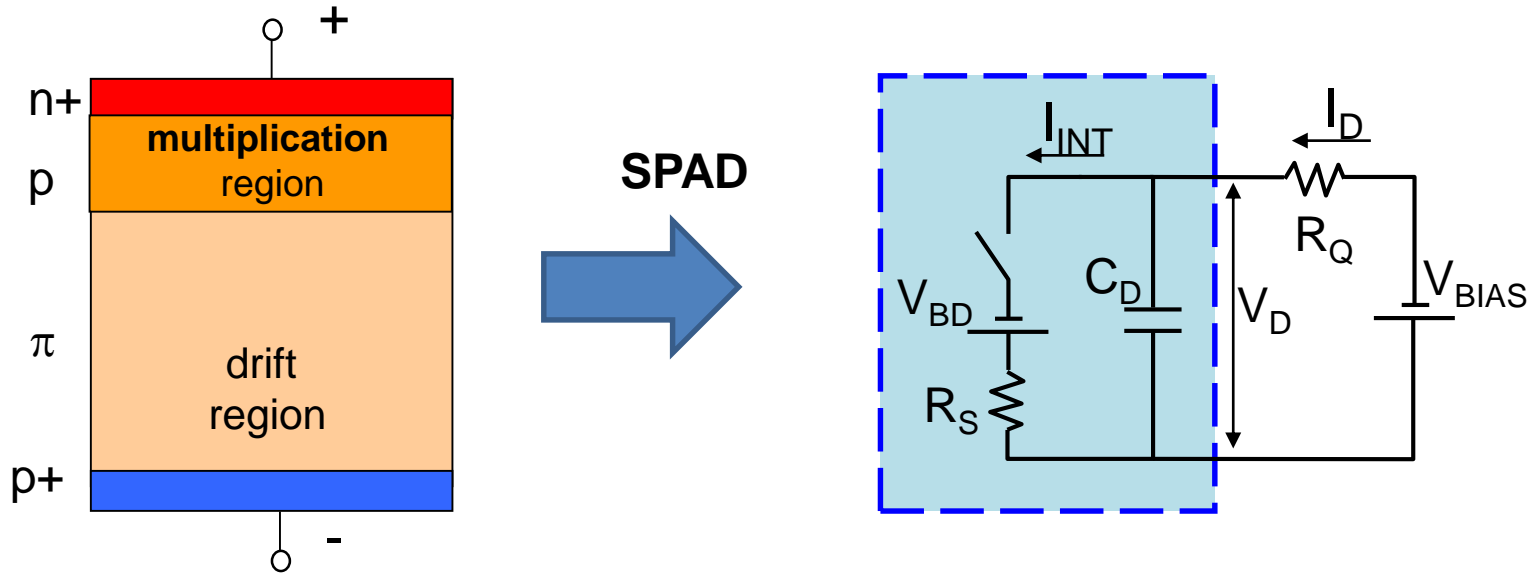
APD



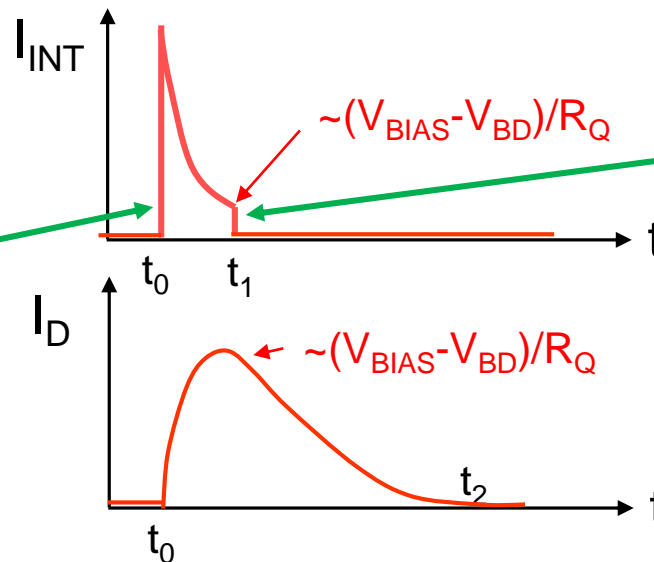
Impact ionization:

- linear mode: gain M
- Geiger mode: avalanche

GM-APD/SPAD: model

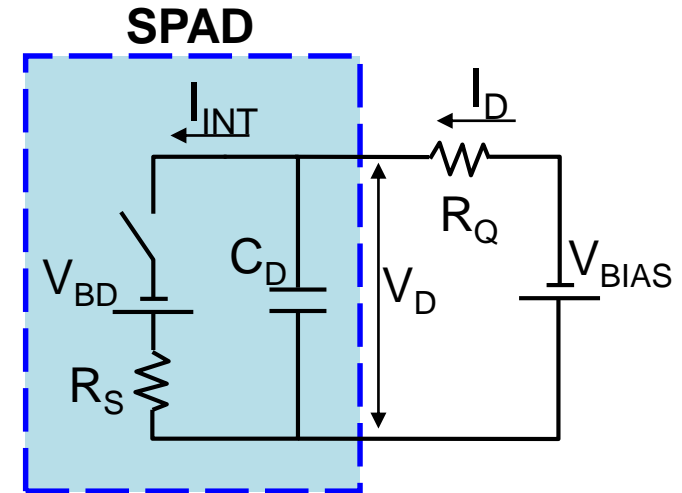
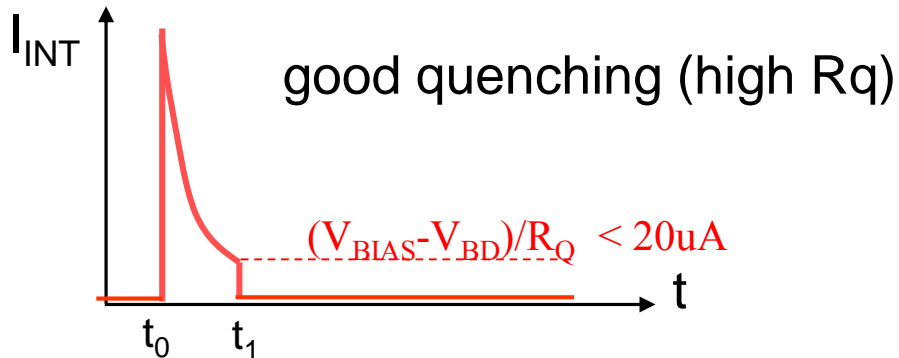
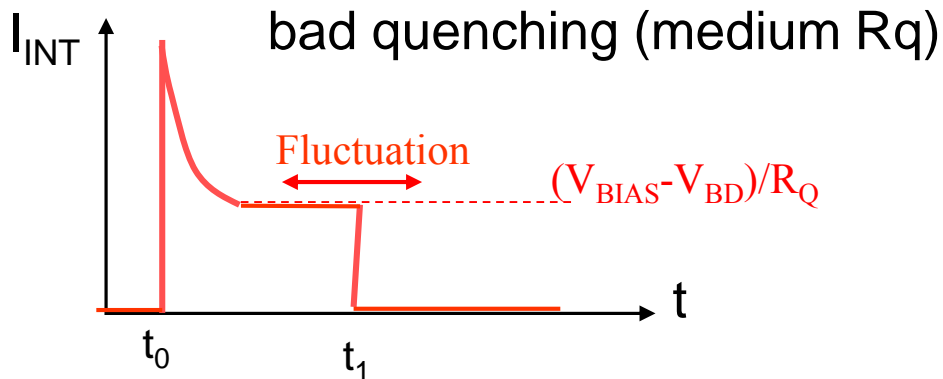
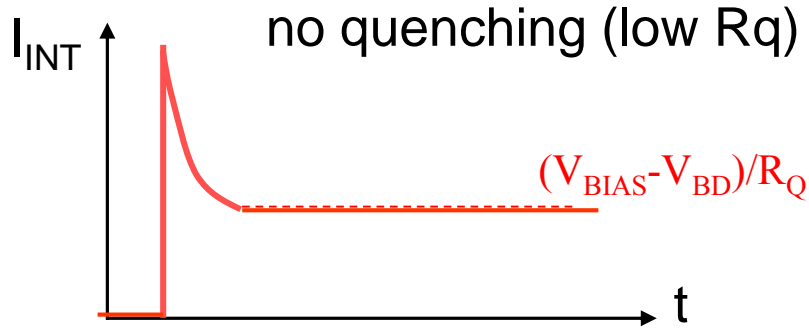


Photon detection:
Avalanche triggering probability



Turn-off probability

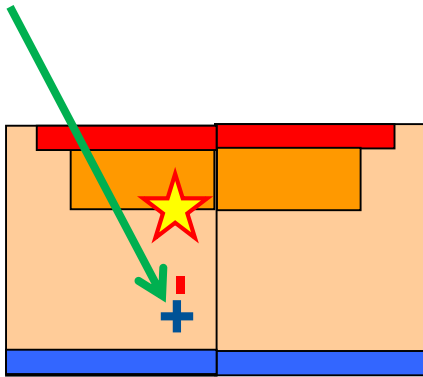
P_{10} – Turn-off probability



fast, efficient!

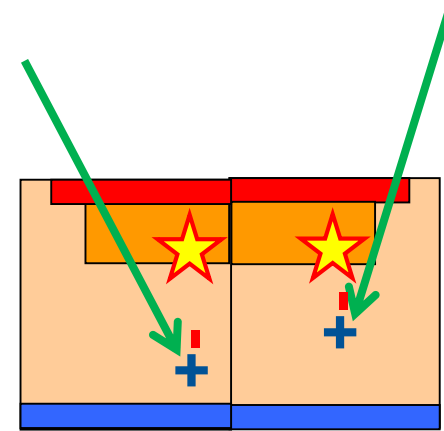
$R_Q > \sim 300 \text{ kohm}$

1 photon

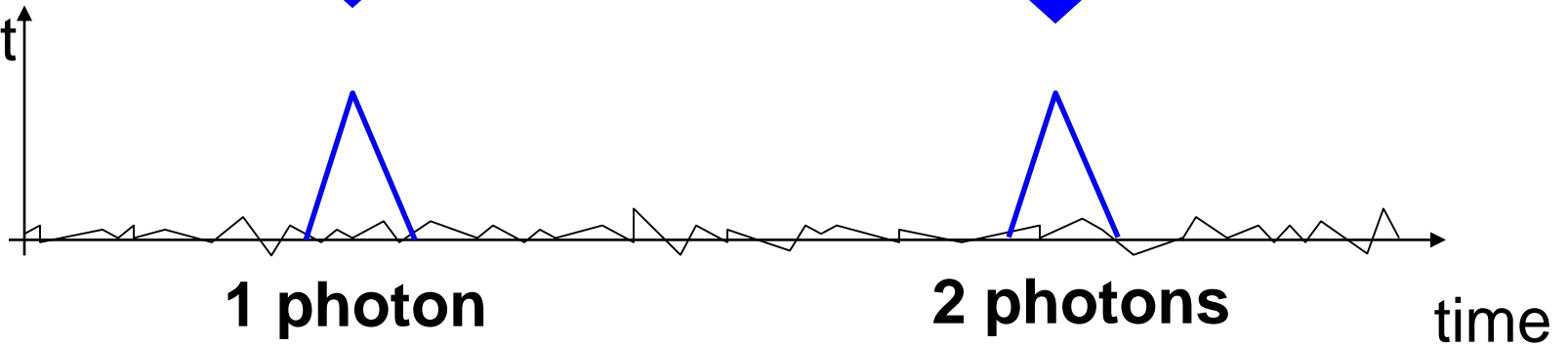


avalanche propagates
all over the diode

2 photons

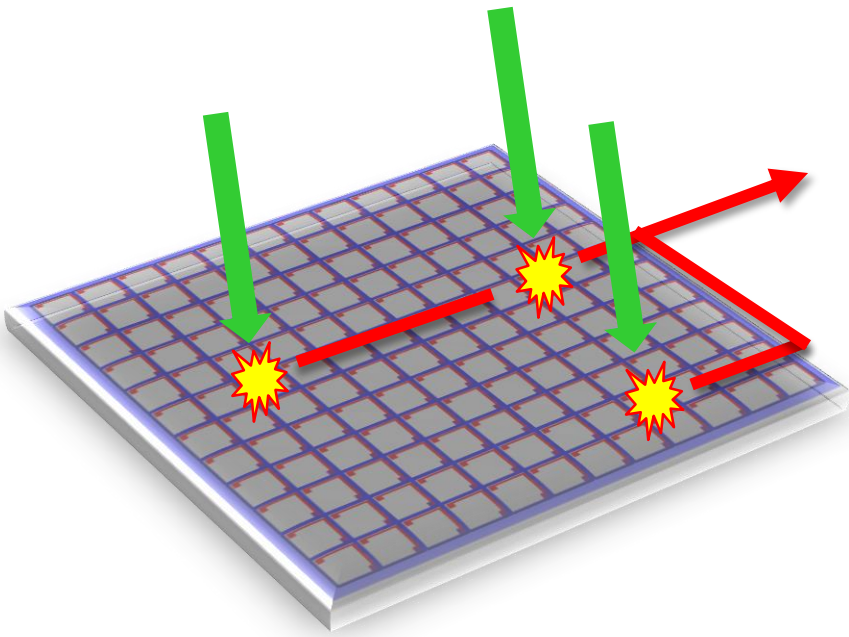


Current



The SPAD response is not proportional to light intensity (in flashes).

SiPM concept



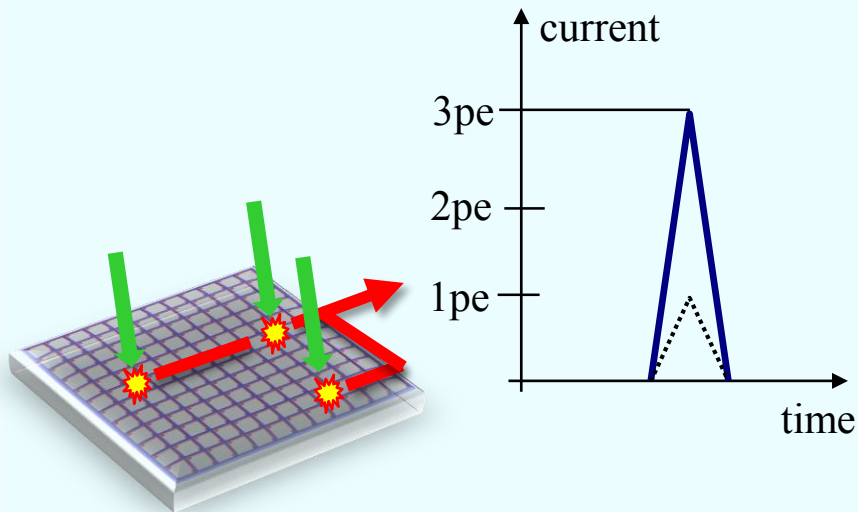
Array of tiny independent SPADs can provide a proportional information.

Analog SiPM

SPADs are connected in parallel.

Output analog signal is proportional to # of photons.

Very simple technology, fully custom, optimized.

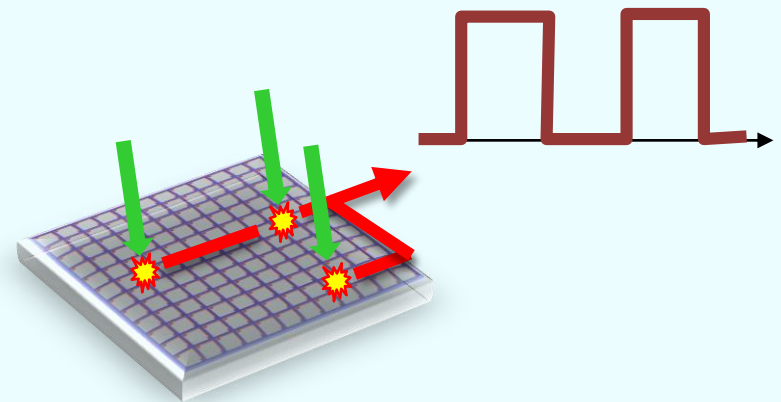


Digital SiPM

Signal digitized at SPAD level.

Integrated Digital architecture produces information on # of photons and time stamp.

Deep sub-mm CMOS technology required.



SPADs/SiPMs: when, where?

1960

Theory of Geiger-mode discharge in pn junctions
 Haitz, McIntyre...

1970

Idea of SPAD exploiting G-M theory
 Various sources

1980

First SPADs
 PoliMI
 EG&G, Canada

Towards picosecond resolution with single-photon avalanche diodes

S. Cova, A. Longoni, and A. Andreoni

Centro Elettronica Quantistica e Strumentazione Elettronica del C.N.R., Politecnico di Milano, Istituto di Fisica, Milano, Italy

(Received 5 August 1980; accepted for publication 17 October 1980)

Some papers from 80-90s:

Avalanche photodiodes and quenching circuits for single-photon detection

S. Cova, M. Ghioni, A. Lacaita, C. Samori, and F. Zappa

1956 APPLIED OPTICS / Vol. 35, No. 12 / 20 April 1996

Photon counting techniques with silicon avalanche photodiodes

Henri Dautet, Pierre Deschamps, Bruno Dion, Andrew D. MacGregor, Darleene MacSween, Robert J. McIntyre, Claude Trottier, and Paul P. Webb

3894 APPLIED OPTICS / Vol. 32, No. 21 / 20 July 1993

SPAD/SiPMs: when, where?

1995

Analog SiPM
concept

Russian researchers

2000+

SPAD & SiPM
developments
in custom and
standard CMOS

few research centers

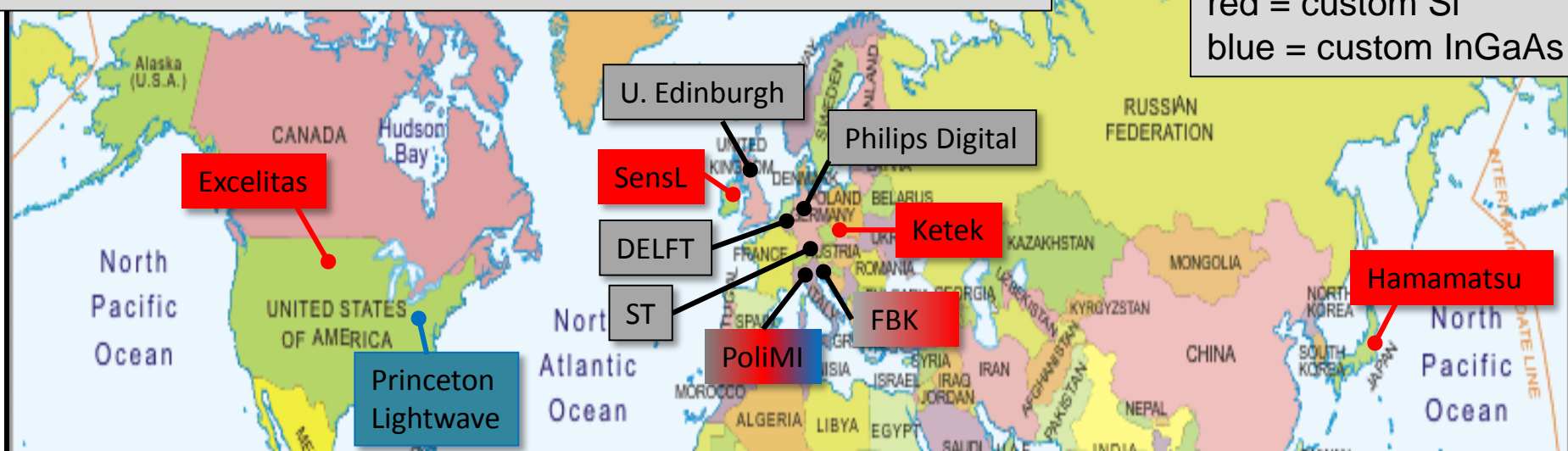
~2005

First SiPM devices
with good
performance

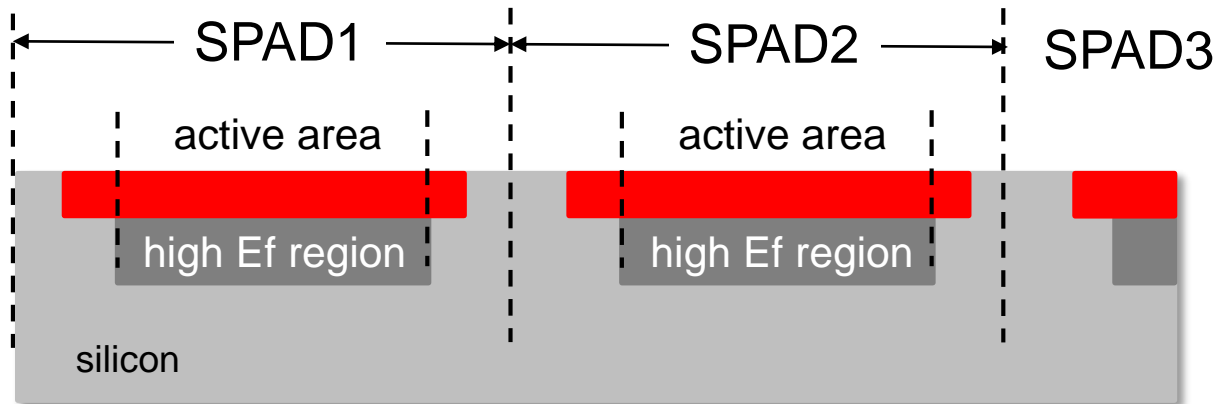
2010+

Growing
industrial
applications

Some of the main actors in SPADs/SiPMs:



...from SPAD to SiPM



New issues:

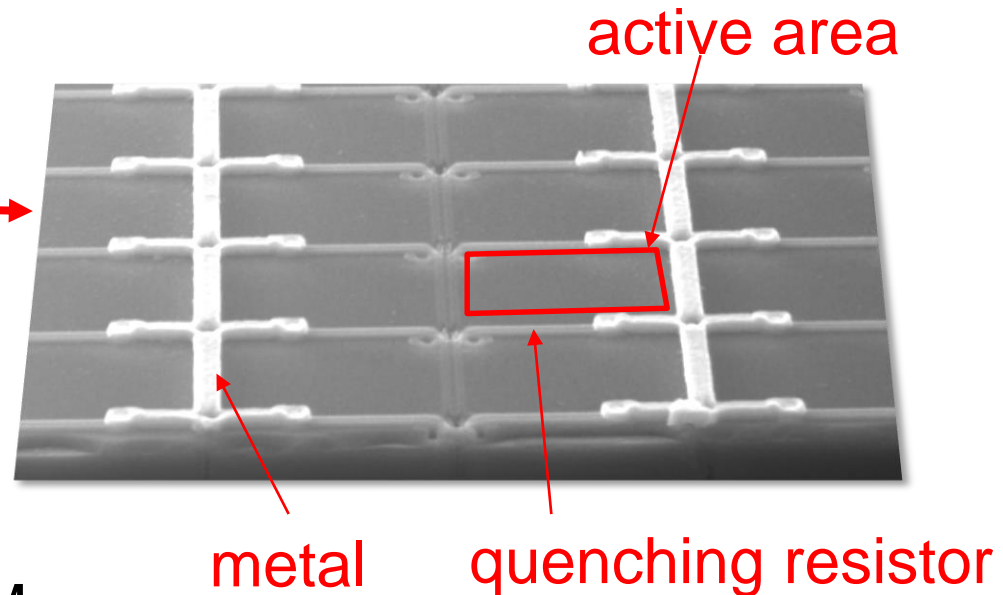
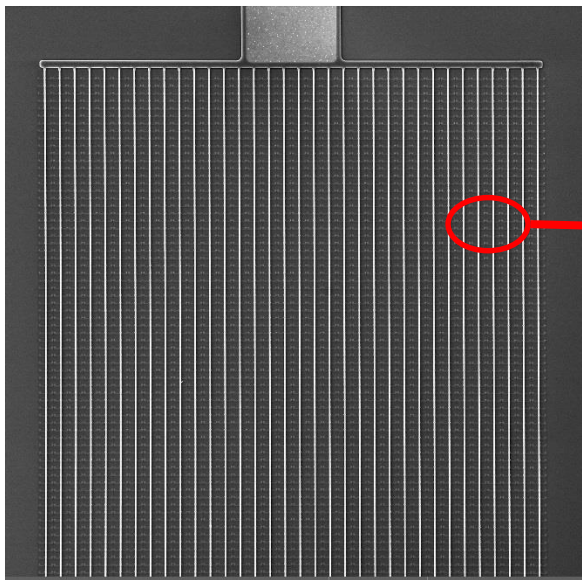
- SPAD fill factor limits the efficiency
- Interactions between SPADs
- Large area



Analog SiPM

Simple technology:

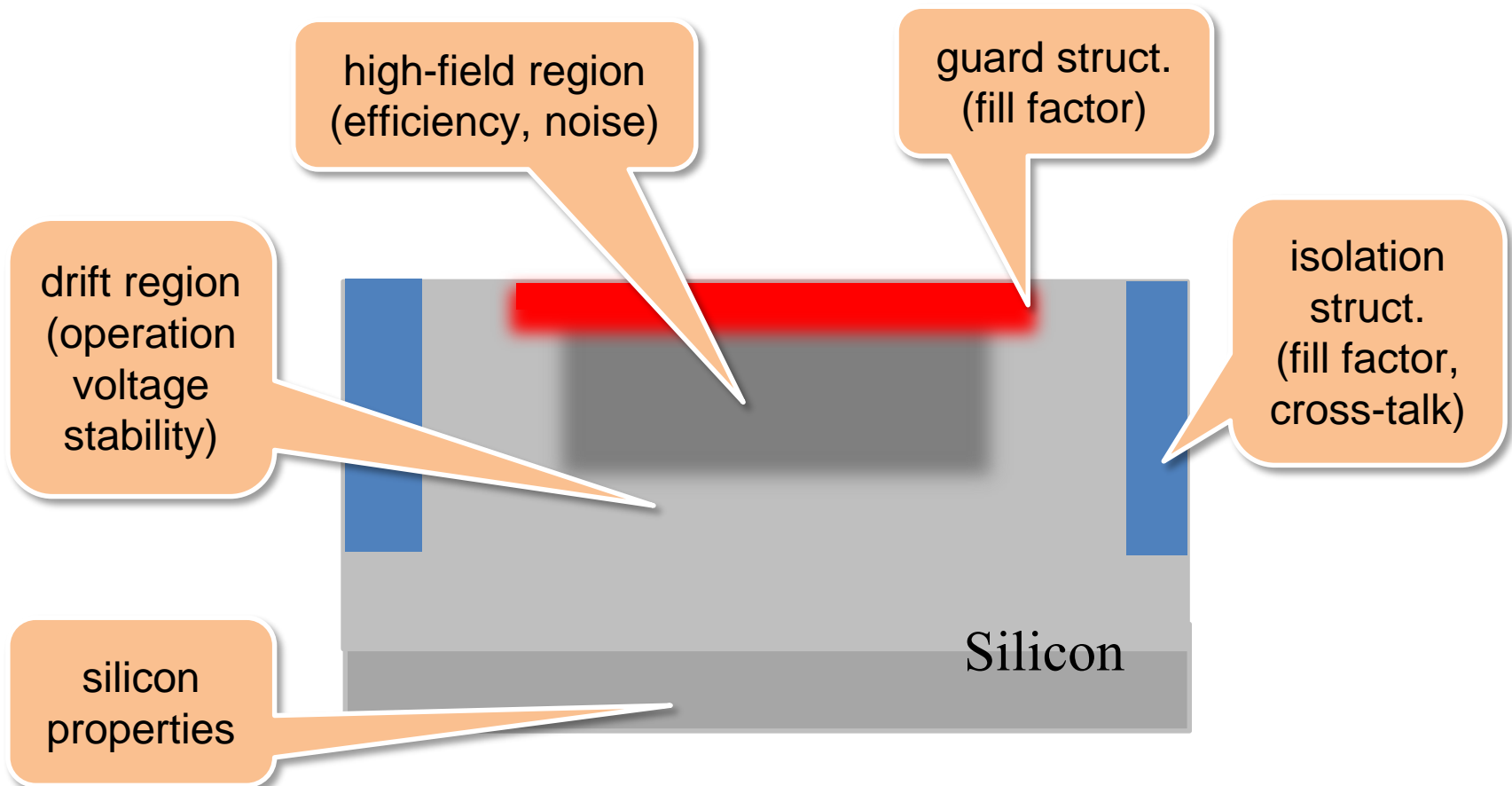
- ~10 lithographic layers
- passive quenching
- «easily» customizable to application



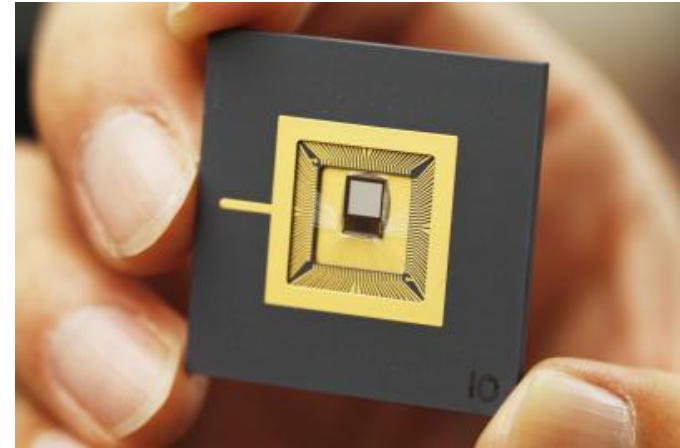
SEM picture of a 1x1mm² SiPM

Analog SiPM

Technology can be optimized in all aspects to get an optimal SPAD.



Digital SiPM

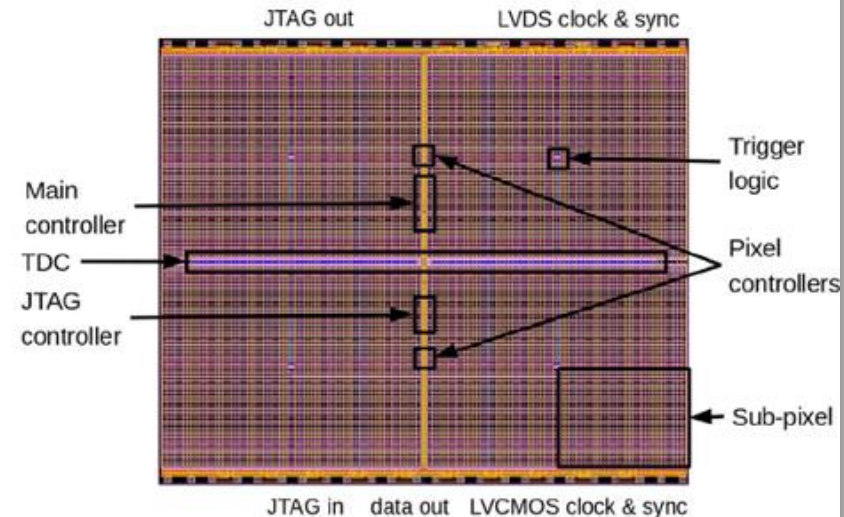
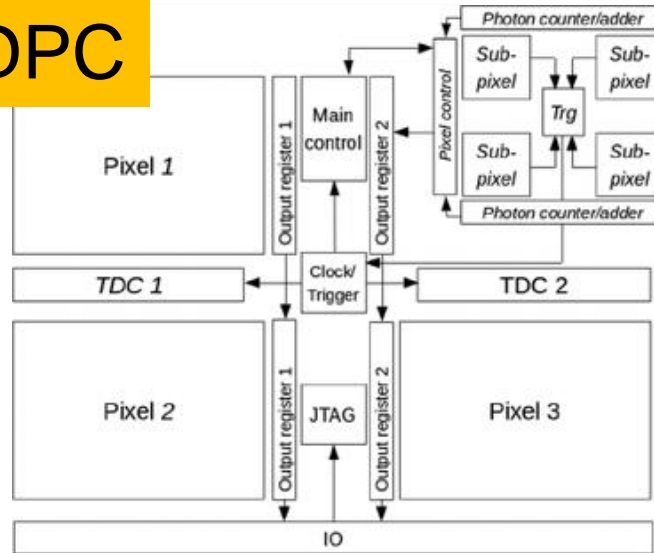


Main Features:

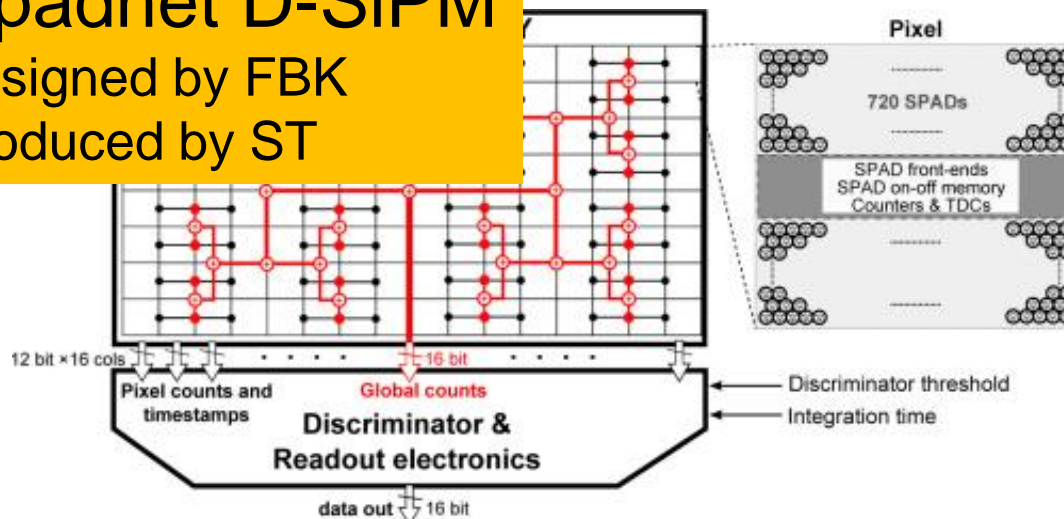
- standard CMOS technology
- integration of «intelligence» in the sensor
 - switch off noisy SPADs
 - distributed TDCs for better timing
 - smart validation systems
 - ...
- architecture is usually customized to the application
- SPAD sensor is sub-optimal

Digital SiPM (for PET) - examples

Philips DPC

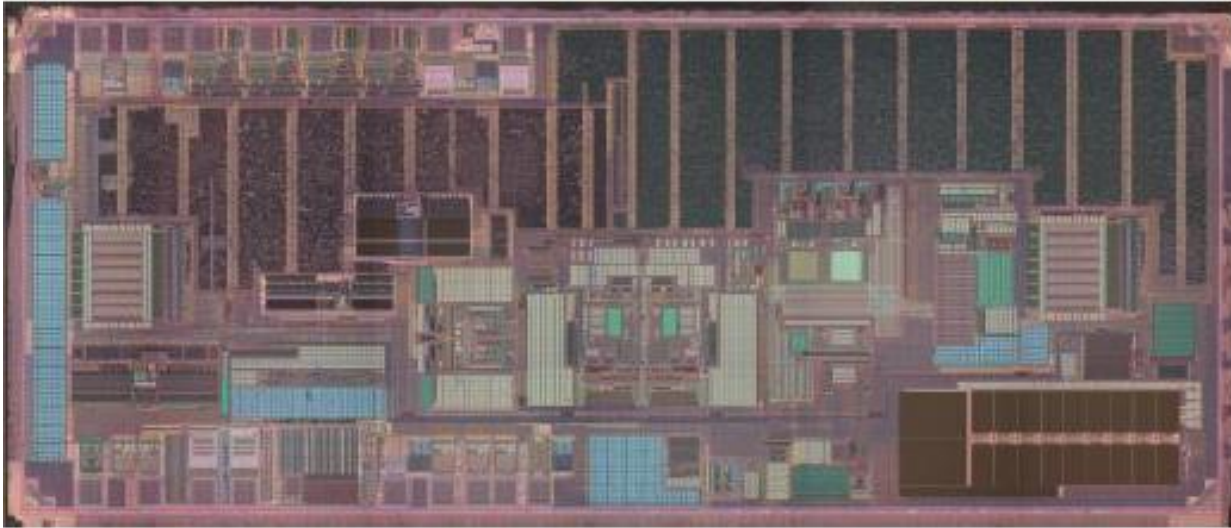


Spadnet D-SiPM designed by FBK produced by ST



From high-end applications to consumer

- STM SPAD-based TOF Proximity Sensor



@Chipworks (<http://ww2.chipworks.com/e/4202/6180-Time-of-Flight-Sensor-pdf/hwvfs/713665047>)

Main characteristics of a SiPM

Parameters of a SiPM

1) Gain

Number of electrons produced per detected photon

2) Primary Noise (Dark Count Rate [Hz])

Cells firing spontaneously

3) Correlated Noise → excess noise factor (ENF)

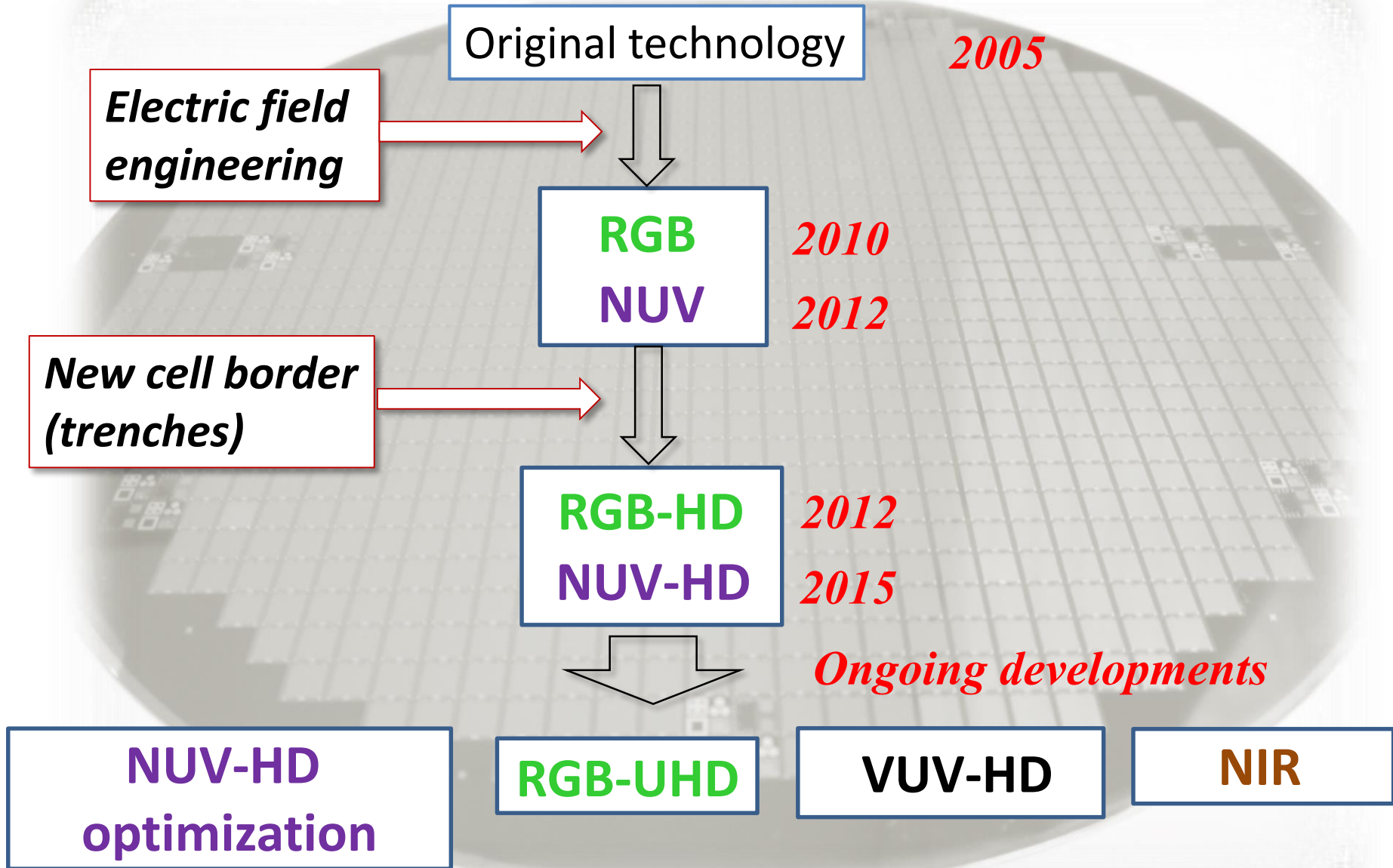
after-pulsing, optical cross-talk

4) Photo-detection efficiency (PDE)

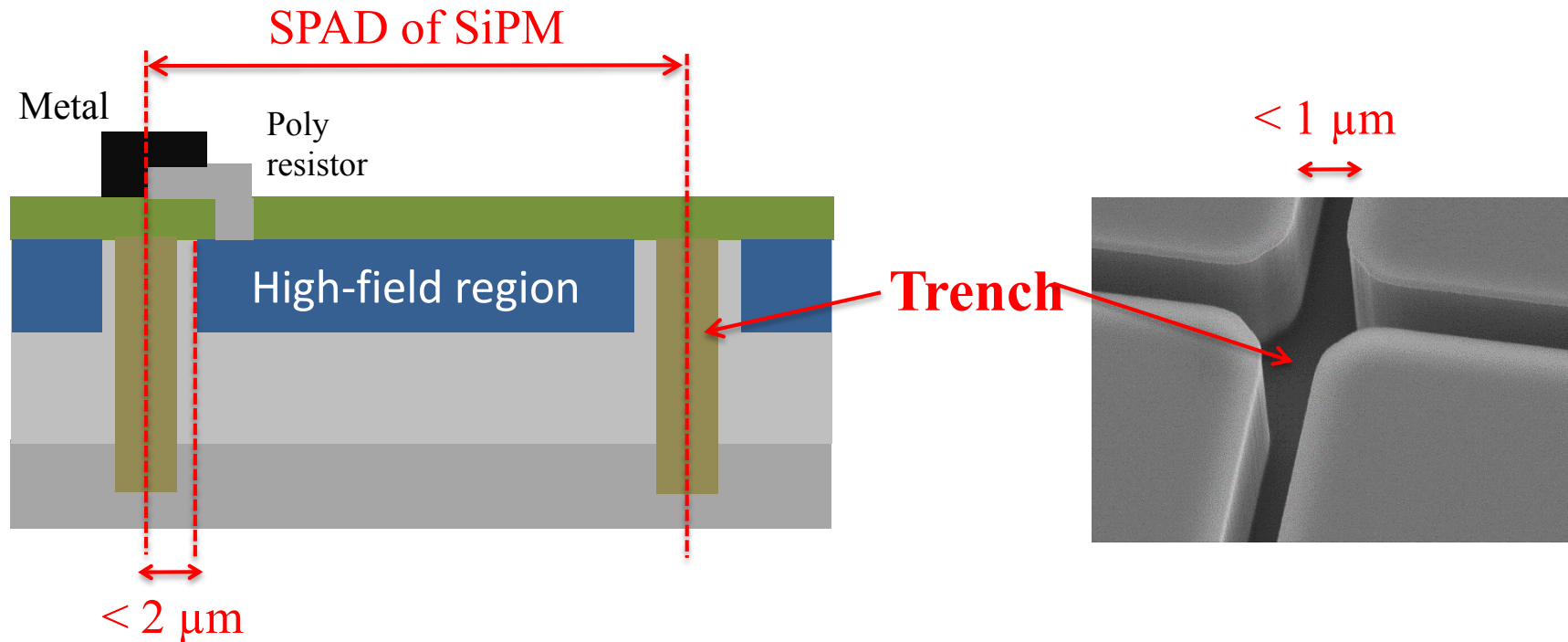
5) Single Photon Time Resolution (SPTR)

Description of each parameter with reference to an FBK technology: NUV-HD

FBK SiPM technology roadmap

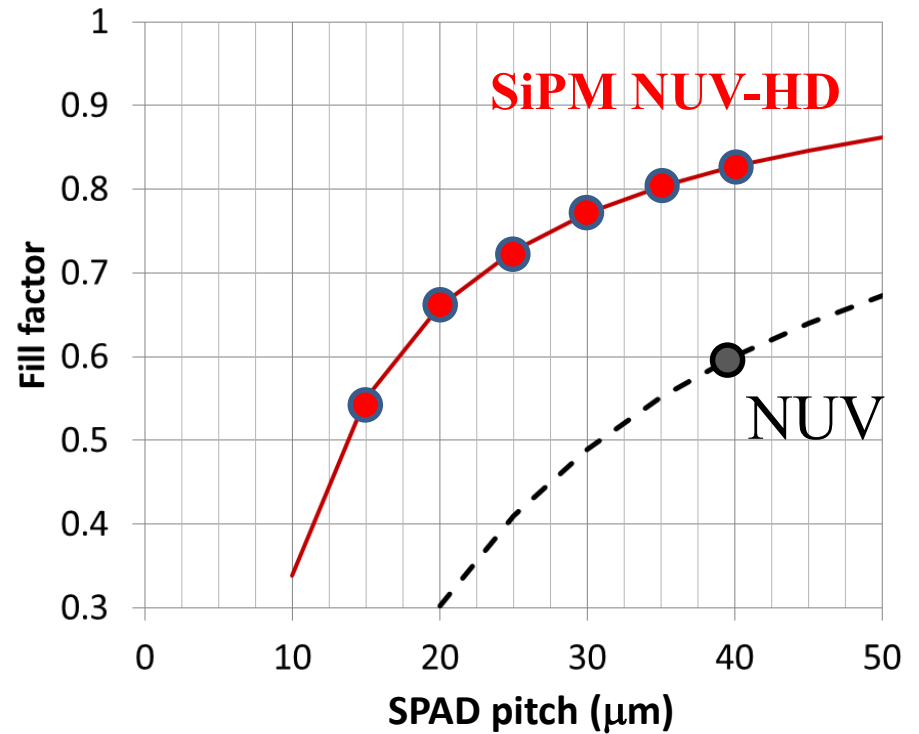
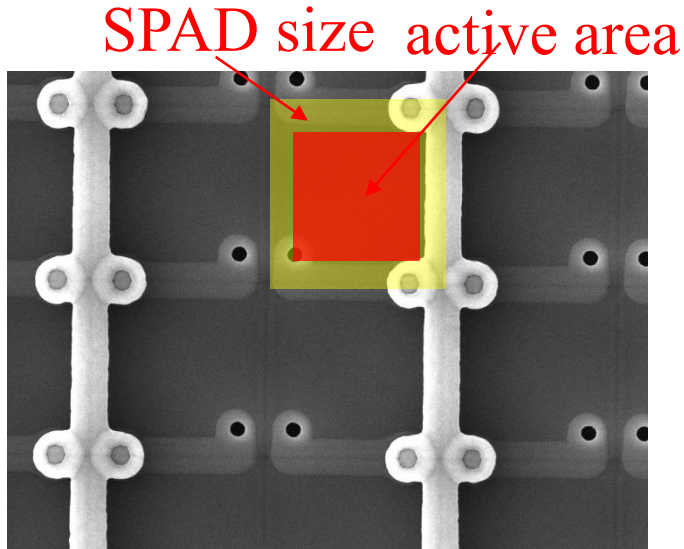


HD technology



- Narrow dead border region \rightarrow High Fill Factor
- Trenches between cells \rightarrow Low Cross-Talk
- Make it simple: 9 lithographic steps

HD: layout features



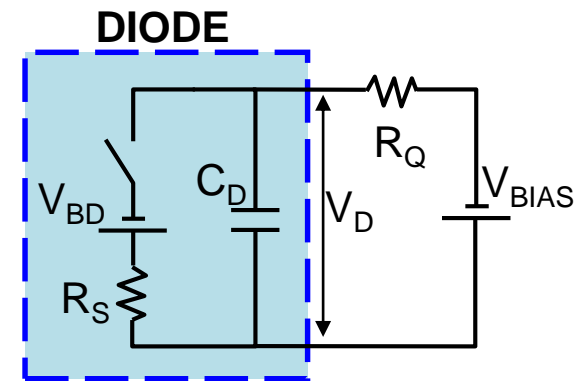
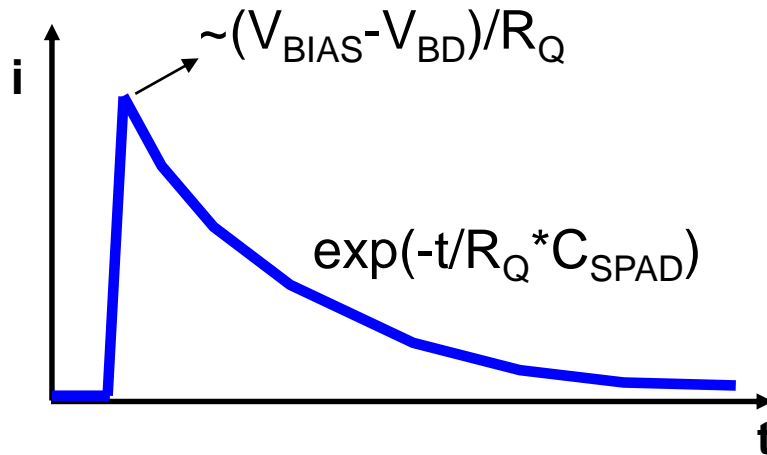
SPAD Pitch	15 μm	20 μm	25 μm	30 μm	35 μm	40 μm
Fill Factor (%)	55	66	73	77	81	83
SPAD/mm ²	4444	2500	1600	1111	816	625

High Dynamic Range

High PDE

Gain of a SPAD/SiPM

Gain = number of electrons per photo-carrier generation

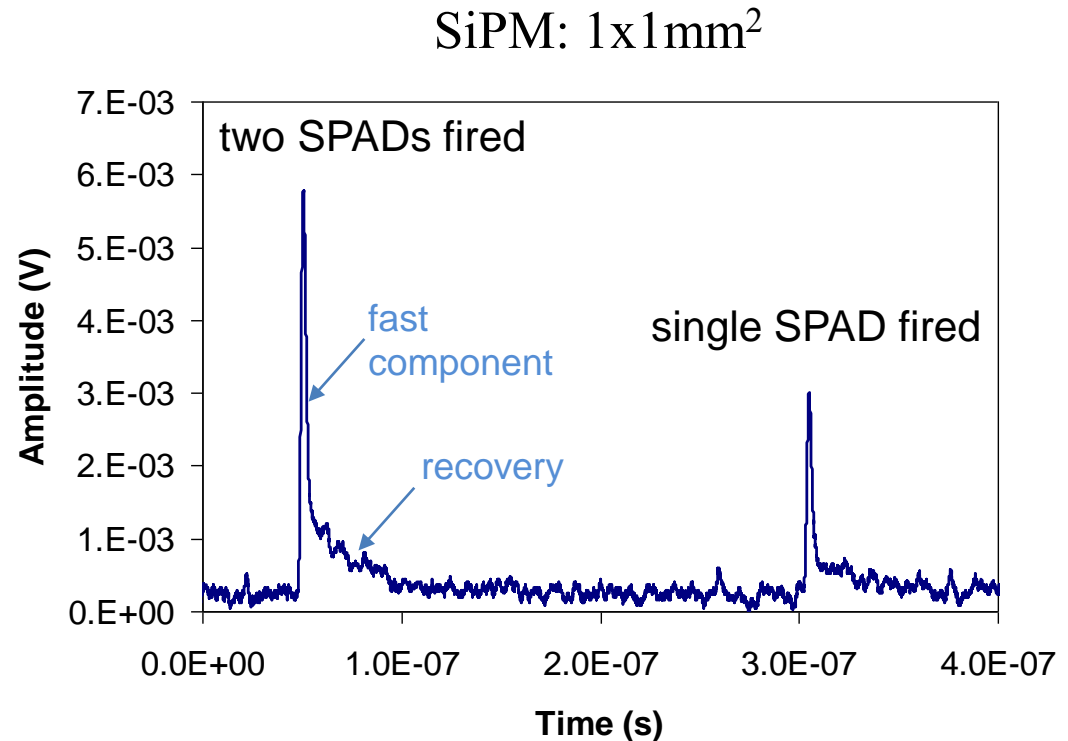
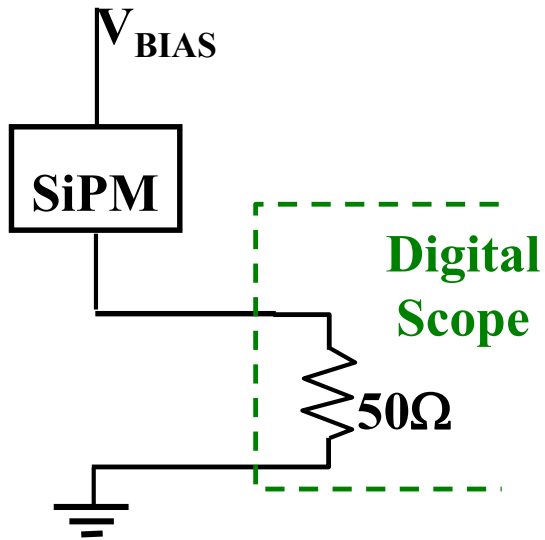


$$\text{Gain} = I_{\text{MAX}} \frac{\tau_Q}{q} = \frac{(V_{\text{BIAS}} - V_{\text{BD}}) * \tau_Q}{R_Q q} = \frac{(V_{\text{BIAS}} - V_{\text{BD}}) * C_D}{q}$$

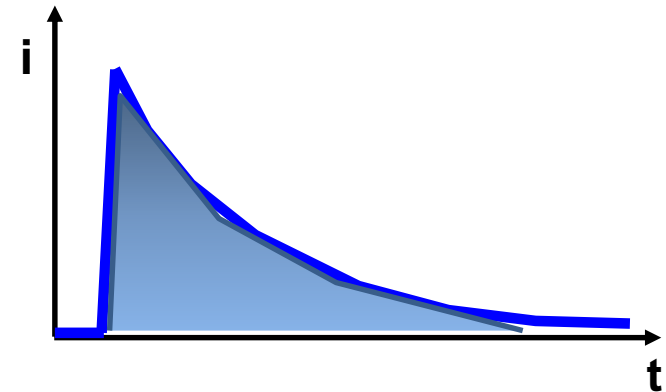
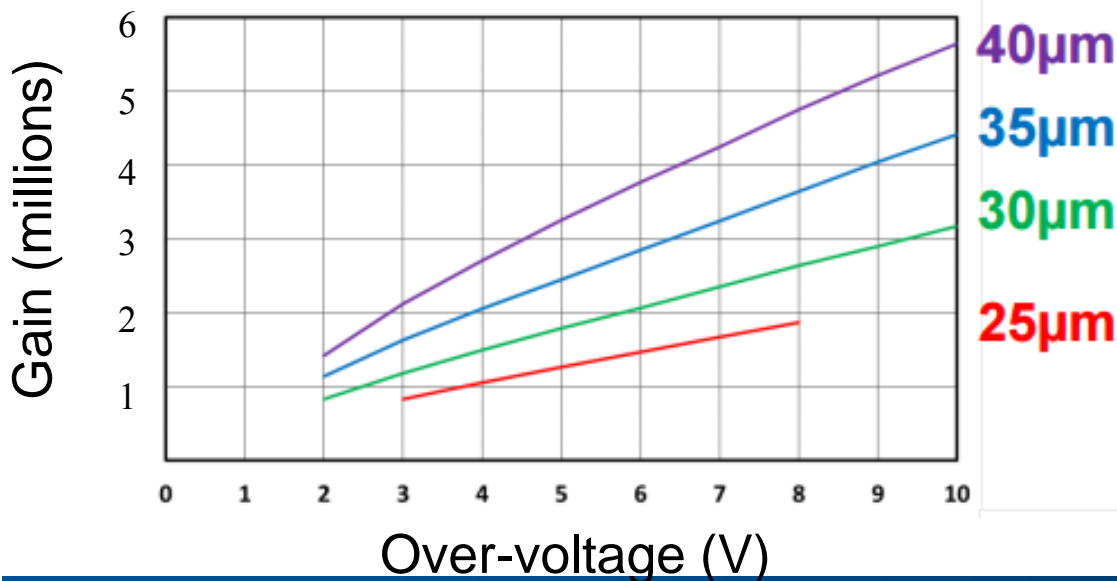
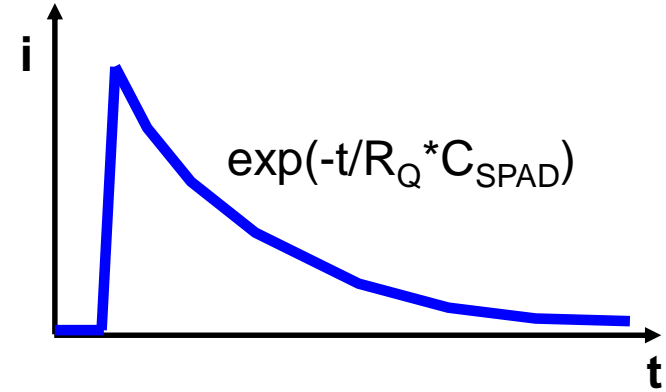
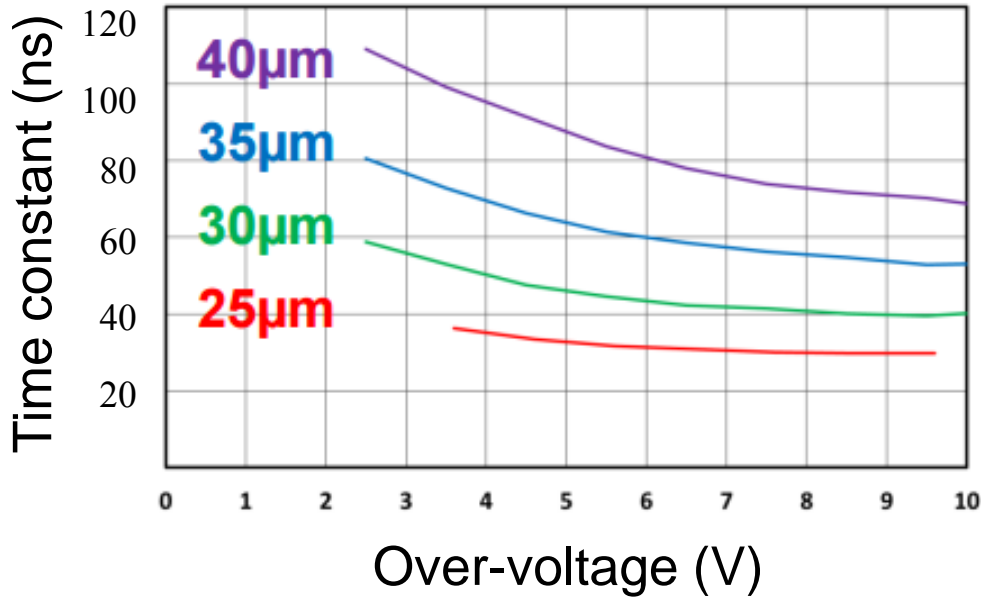
Uniformity and stability of V_{BD} is crucial!

SiPM Signal – NO amplifier

Thanks to the large gain it is possible to connect the SiPM directly to the scope



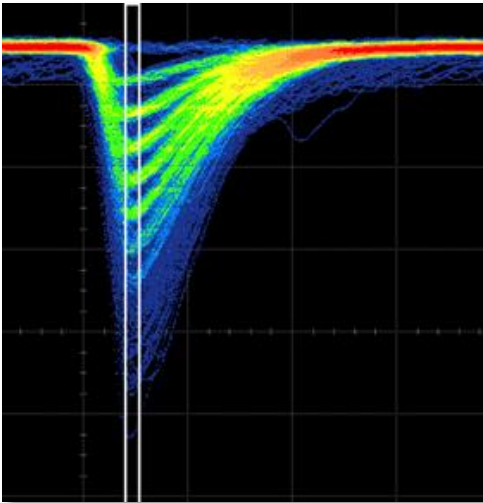
Gain of a NUV-HD SiPM



SiPM photon counting capability

→ gain uniformity in SPAD and SPAD-to-SPAD

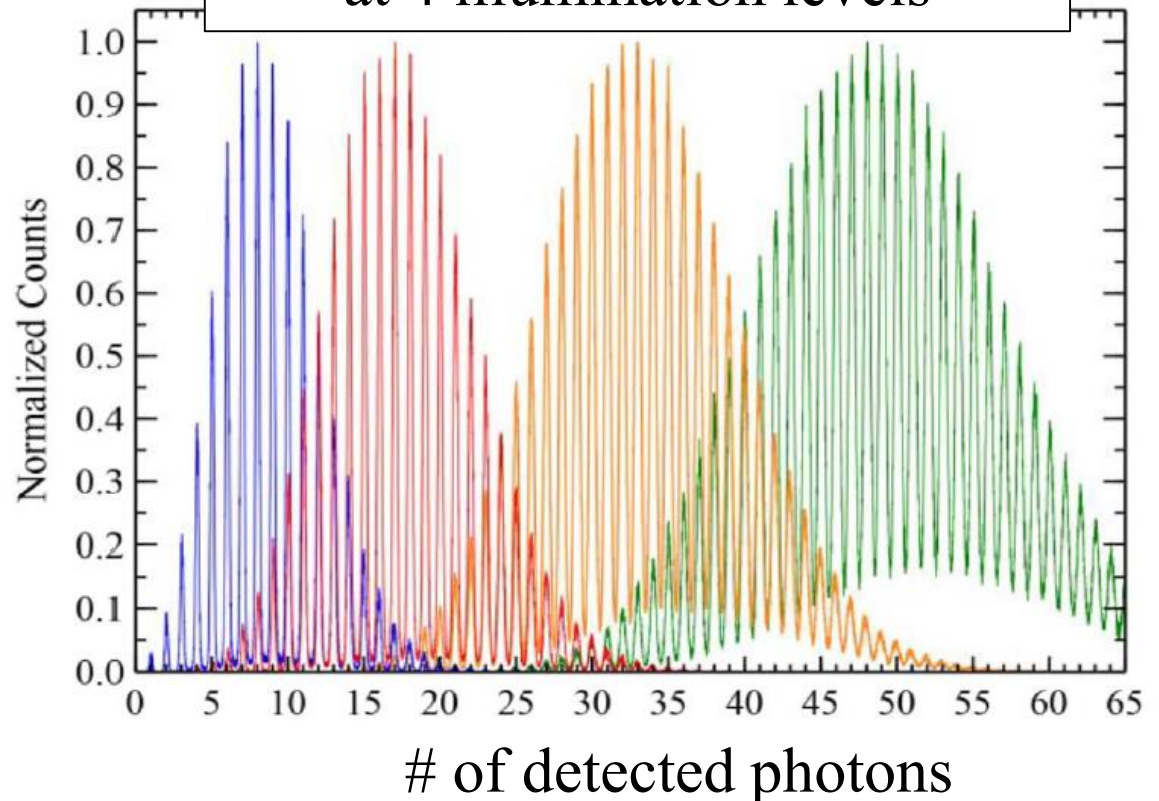
SiPM illuminated
with weak pulses



T = 20 C

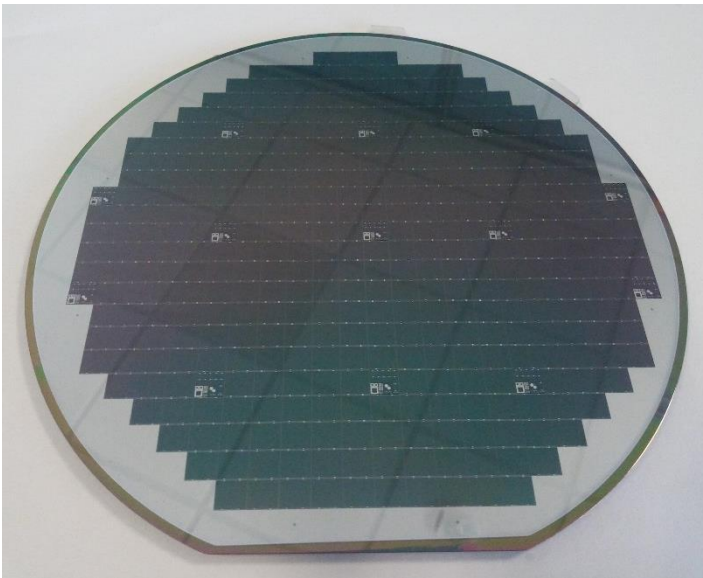
SiPM area 1x1mm²

Histogram of the signal area
at 4 illumination levels



V_{BD} Uniformity

Gain uniformity (intra- and inter- device) is mostly affected by V_{bd} . What is the V_{bd} uniformity?



6" Silicon wafer

1532 3x3mm² SiPMs per wafer

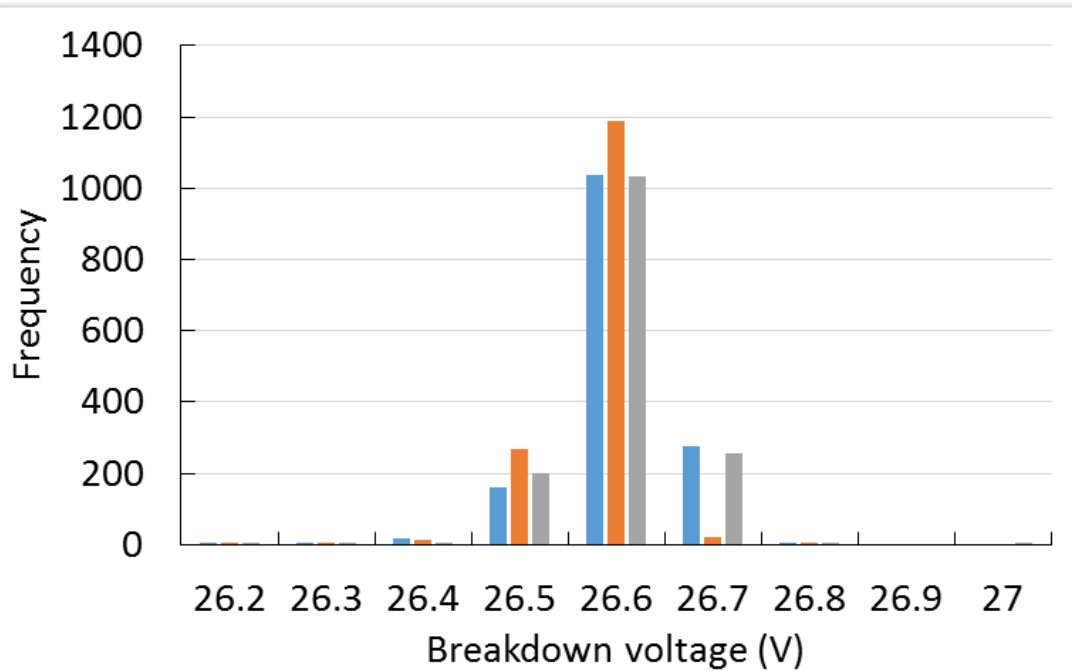
SPAD pitch is **35mm**

Each SiPM has **6295 SPADs**

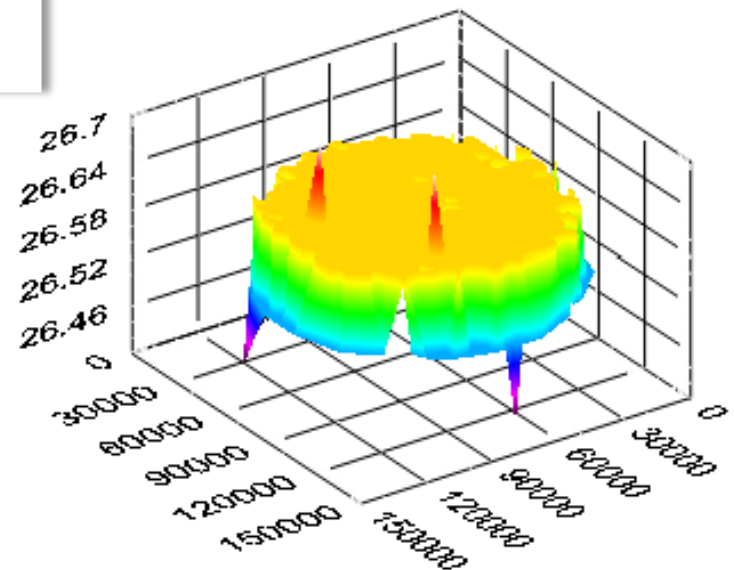
Reverse IV measurement on all
SiPMs on 3 sample wafers:

→ Breakdown voltage

V_{BD} Uniformity

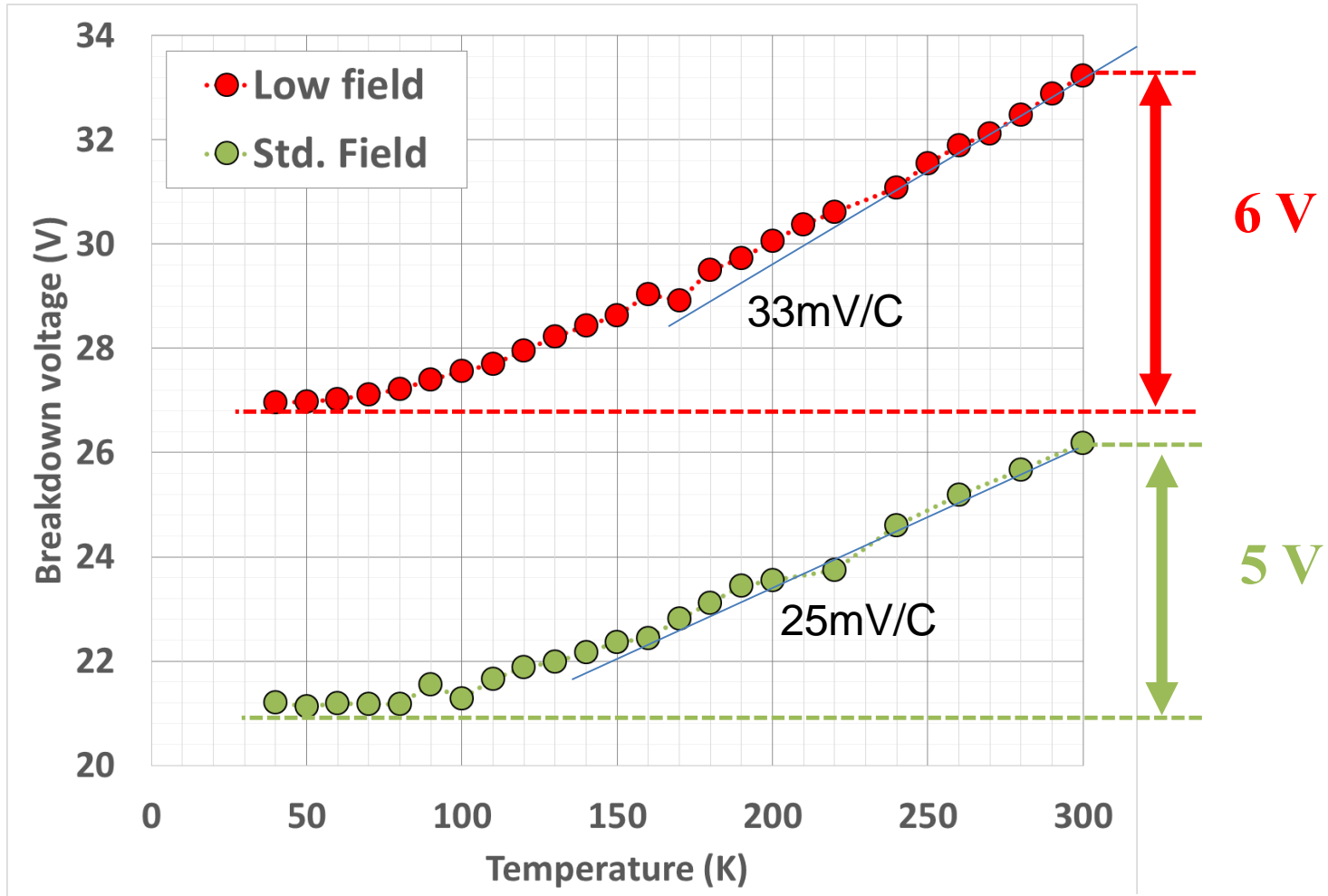


Distribution of V_{BD} on three wafers.
Max variation 200mV!



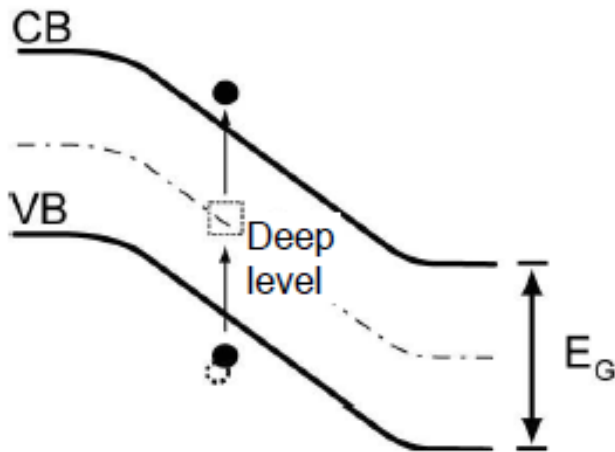
V_{BD} Temperature dependence

The **mean free path** of the carriers in the high-field region increases with decreasing temperature.



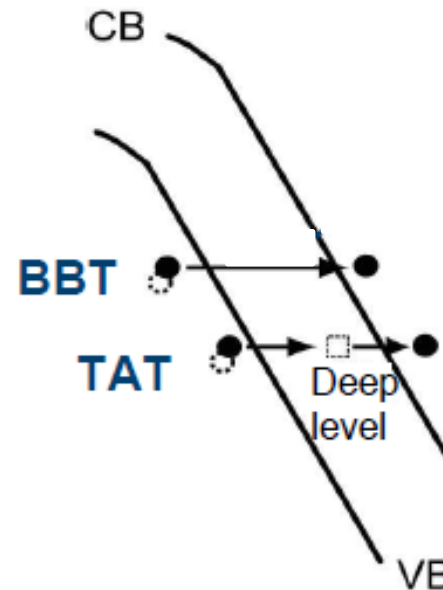
Dark count rate

Thermal generation (SRH model)



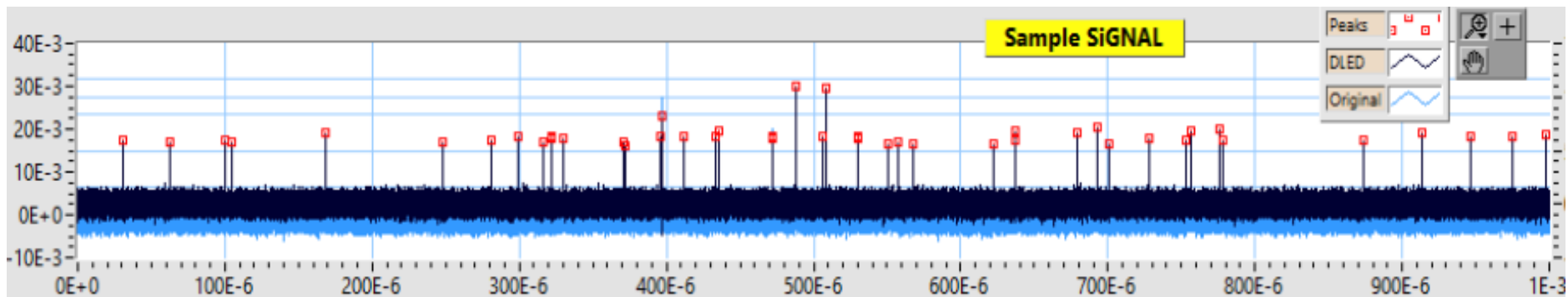
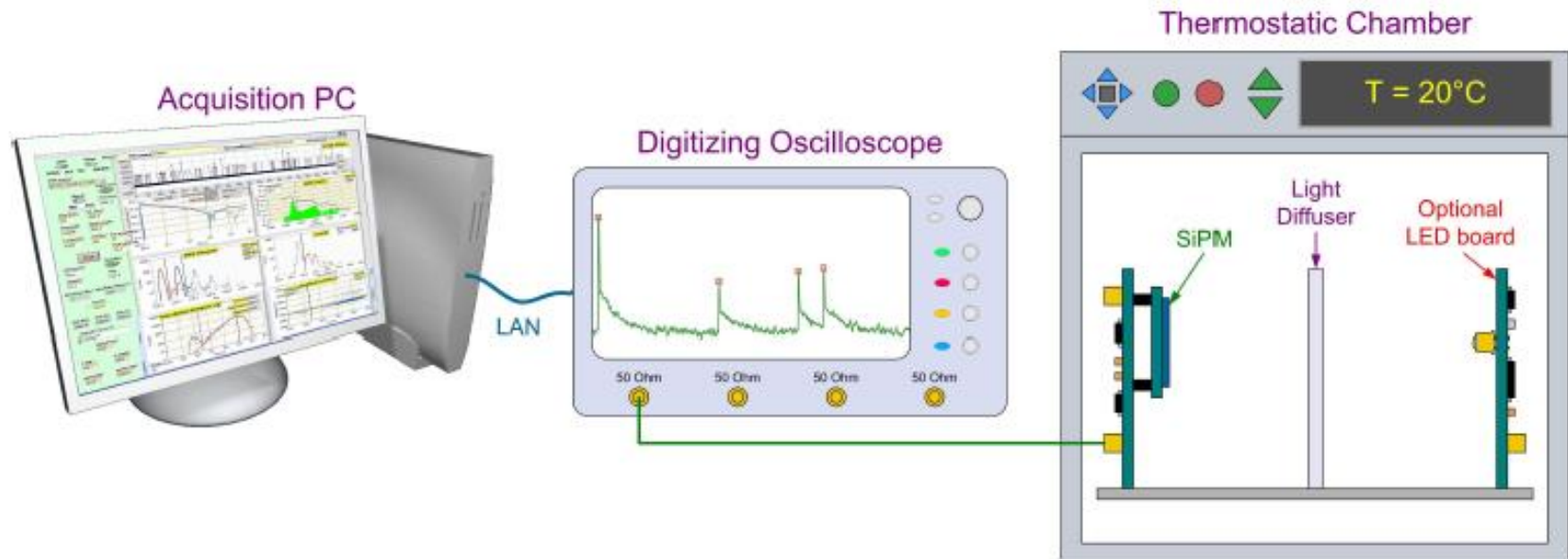
Main source of carrier generation in silicon at room T in standard photodiodes

Tunneling generation



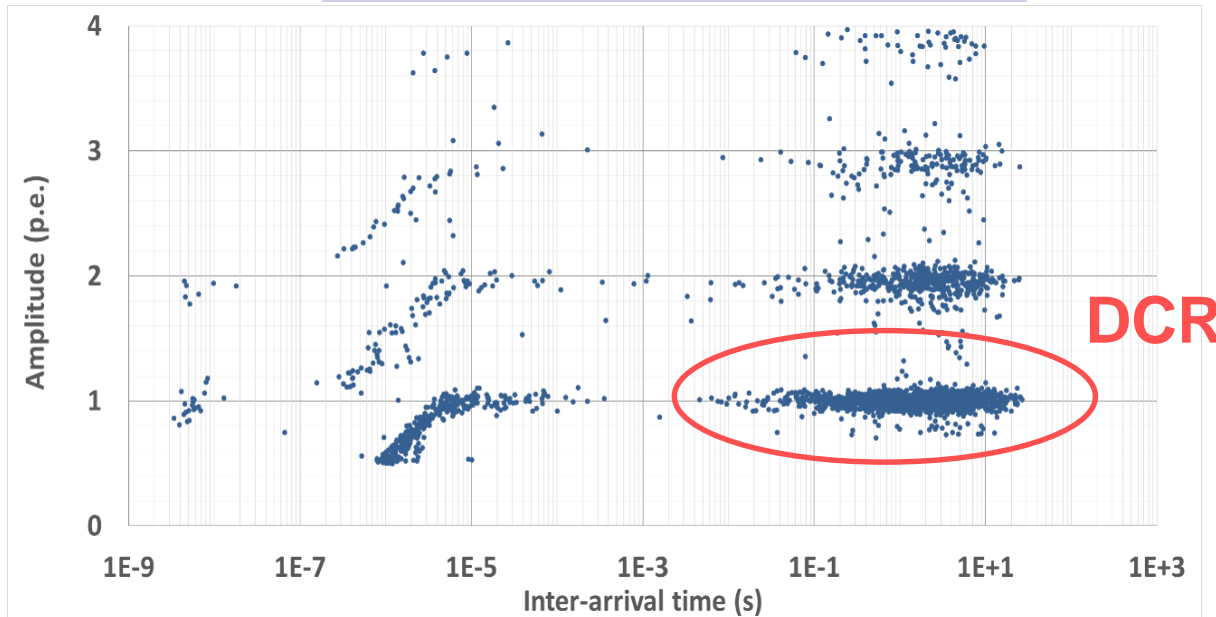
TAT is an important additional contribution in devices relying on impact ionization

DCR measurement



DCR measurement

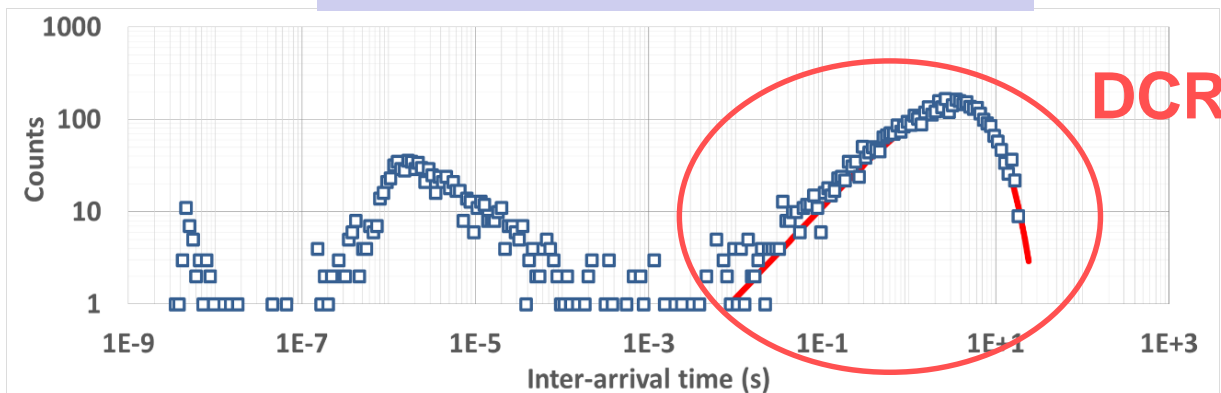
Scatter plot



T=70K
(example to separate well the components)

Scatter plot of amplitude vs inter-times

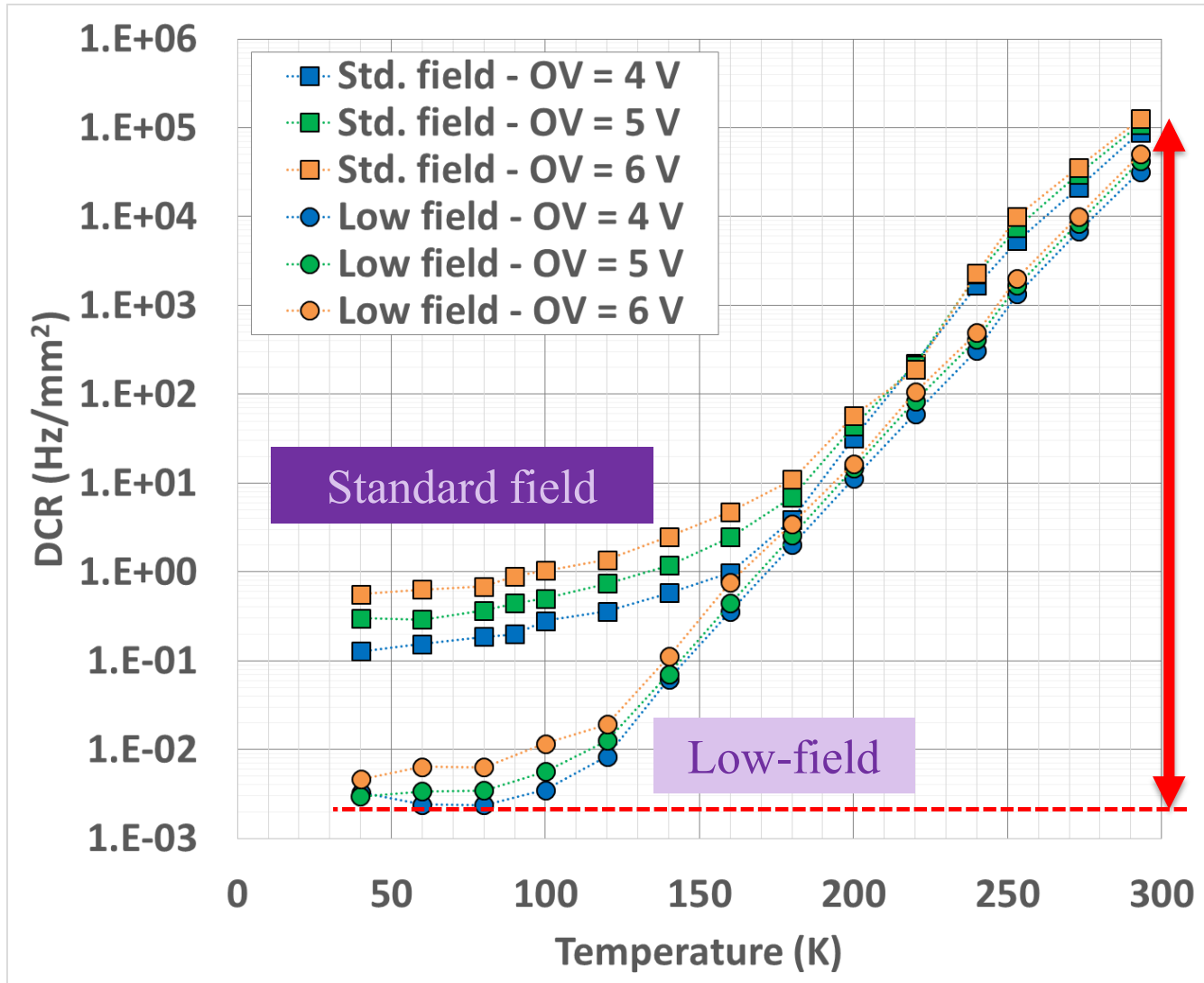
Inter-arrival time histogram



DCR event distribution with Poisson fit

DCR / mm² vs. Temperature

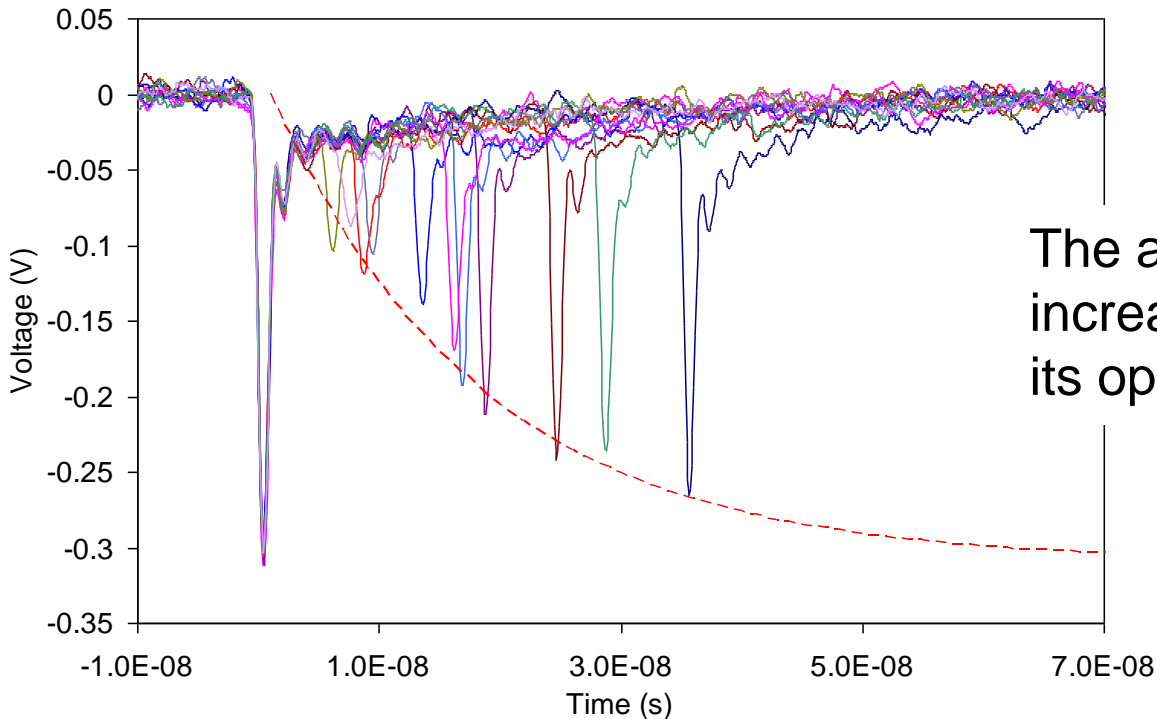
NUV-HD 4x4mm² size 25μm SPAD pitch (25600 SPADs)



After-pulsing Probability

Carriers may be trapped during an avalanche, released and may triggering another avalanche.

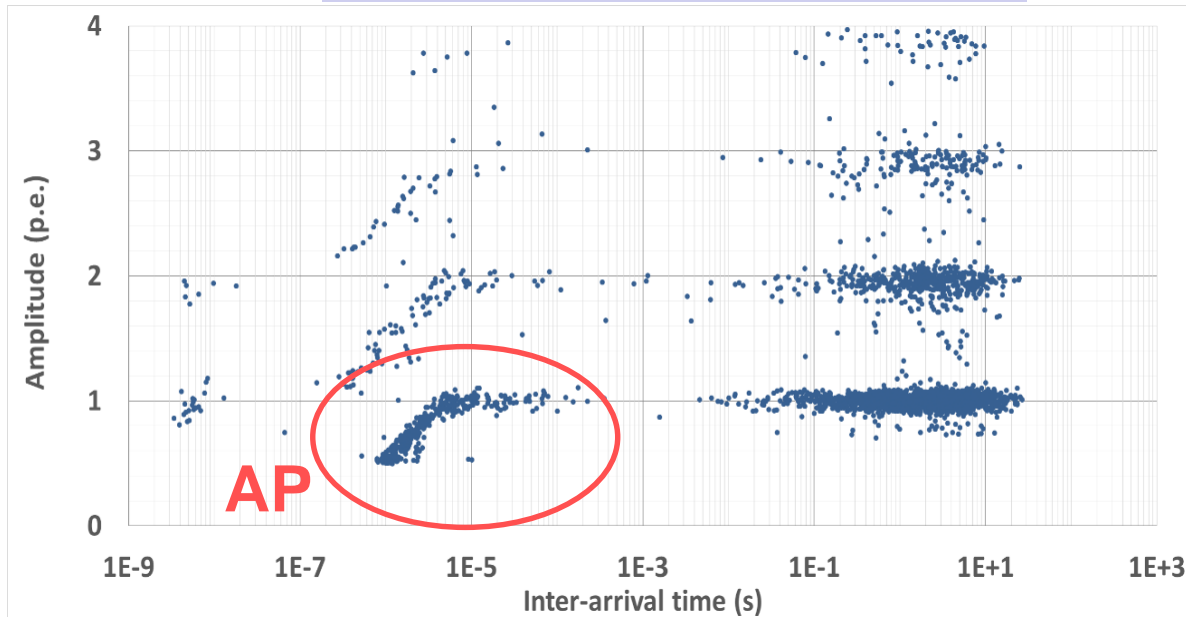
Collection of primary Events with after-pulse



The amplitude of the after-pulse increases as the cell recovers to its operational condition

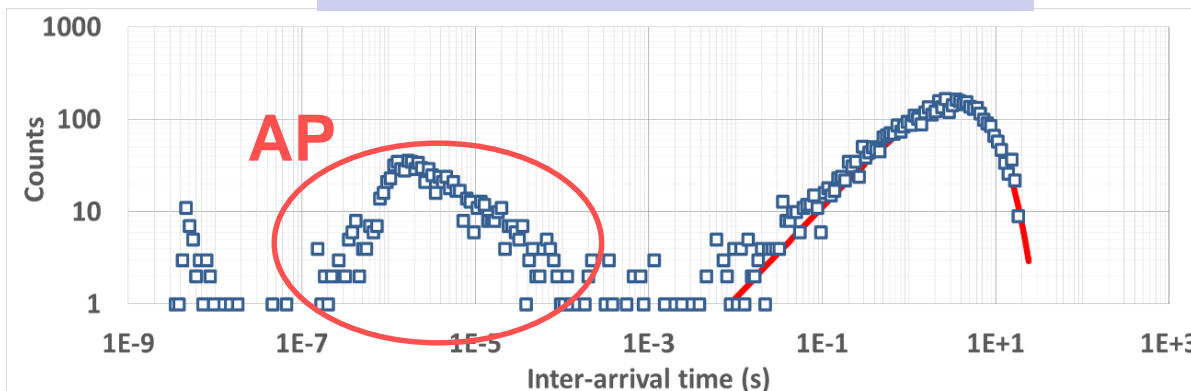
AP measurement

Scatter plot



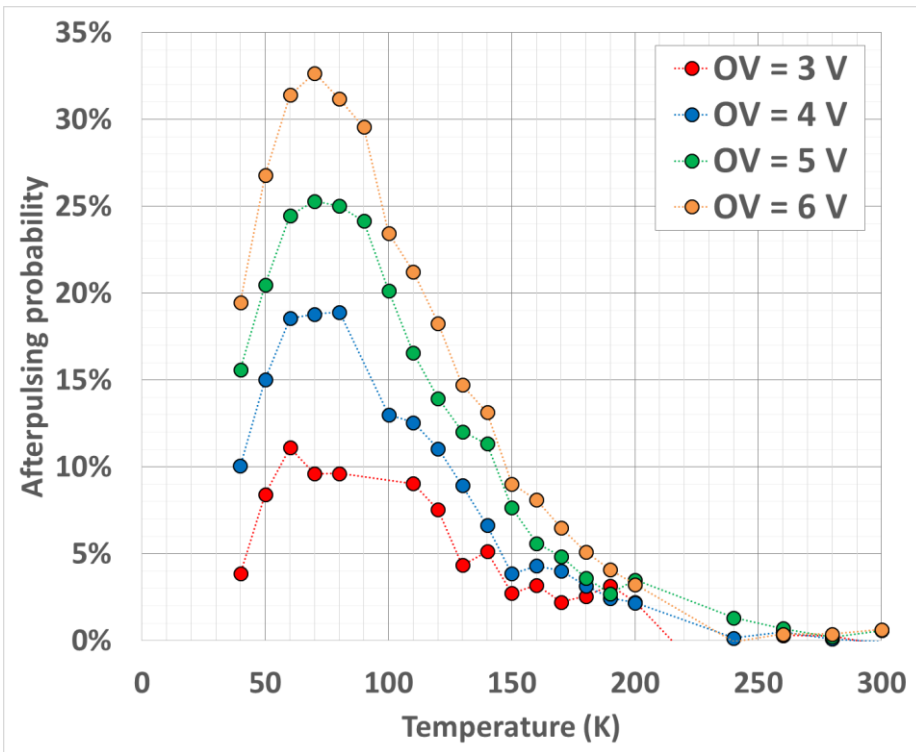
Scatter plot
of amplitude vs
inter-times

Inter-arrival time histogram

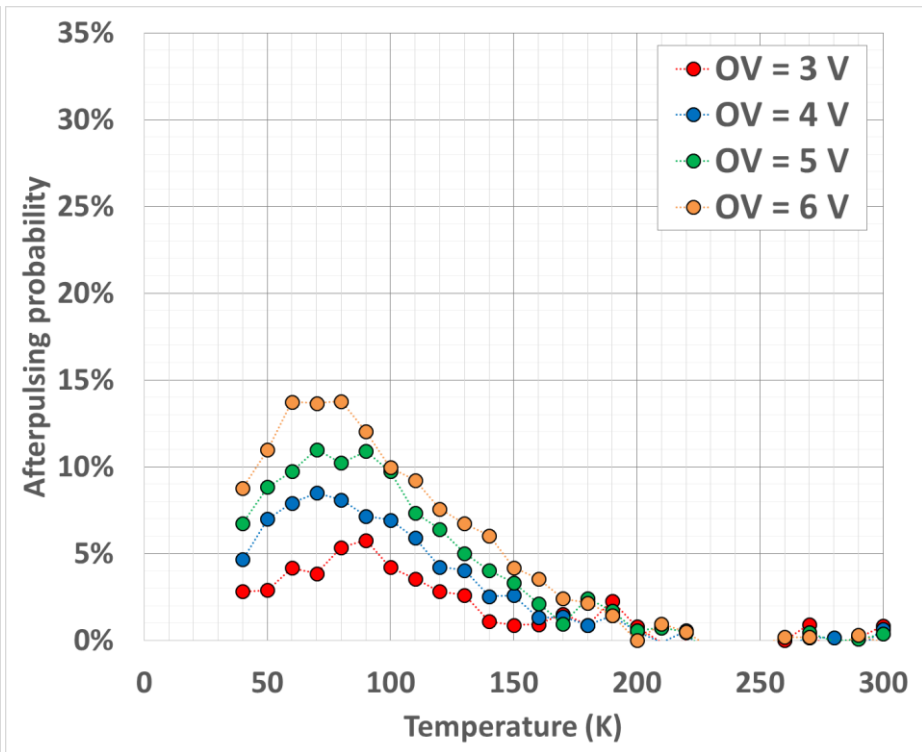


AP in NUV-HD

AP increases with decreasing temperature because the release becomes slower..



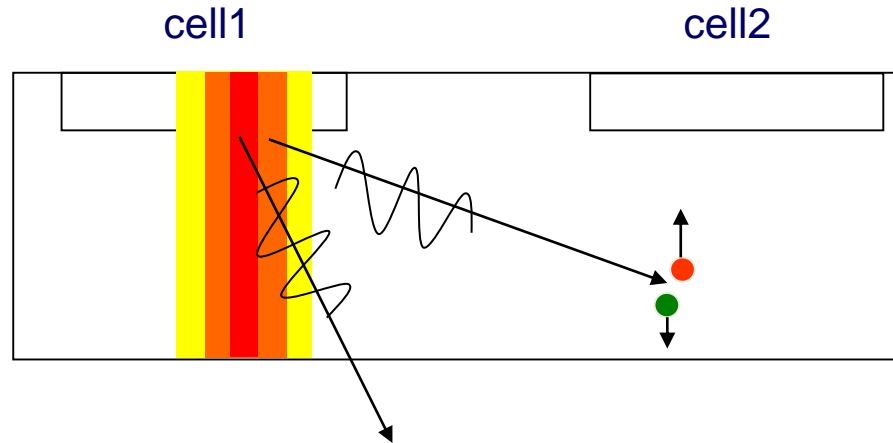
Standard field



Low-field

Optical cross-talk

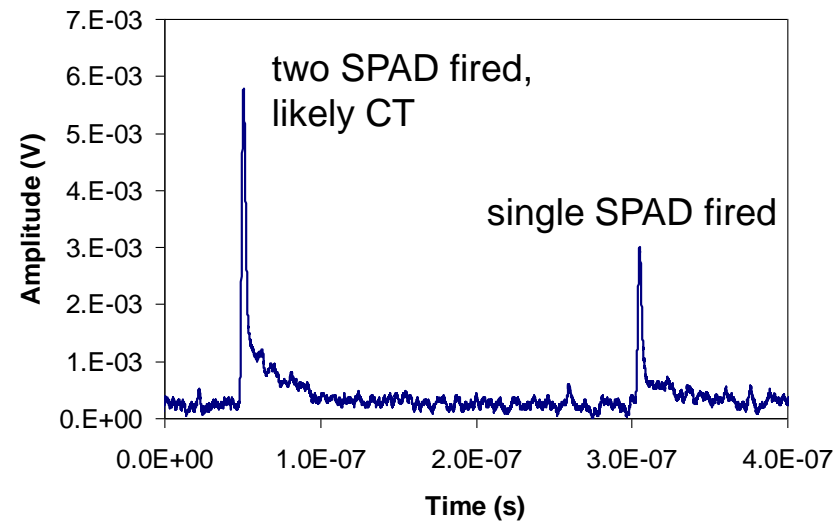
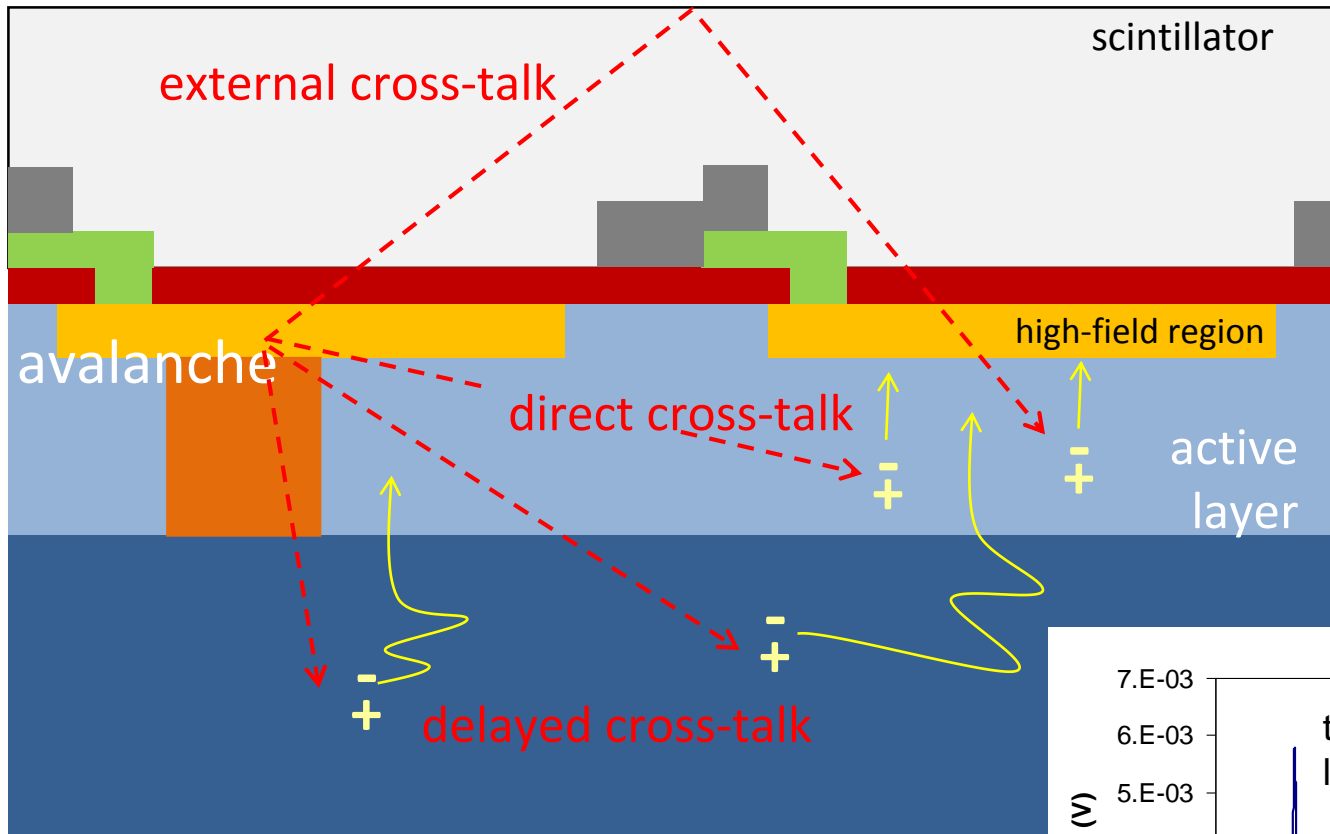
Photons are emitted during an avalanche which may trigger another avalanche in another SPAD



3×10^{-5} photons with energy higher than 1.14eV emitted per carrier crossing the junction.

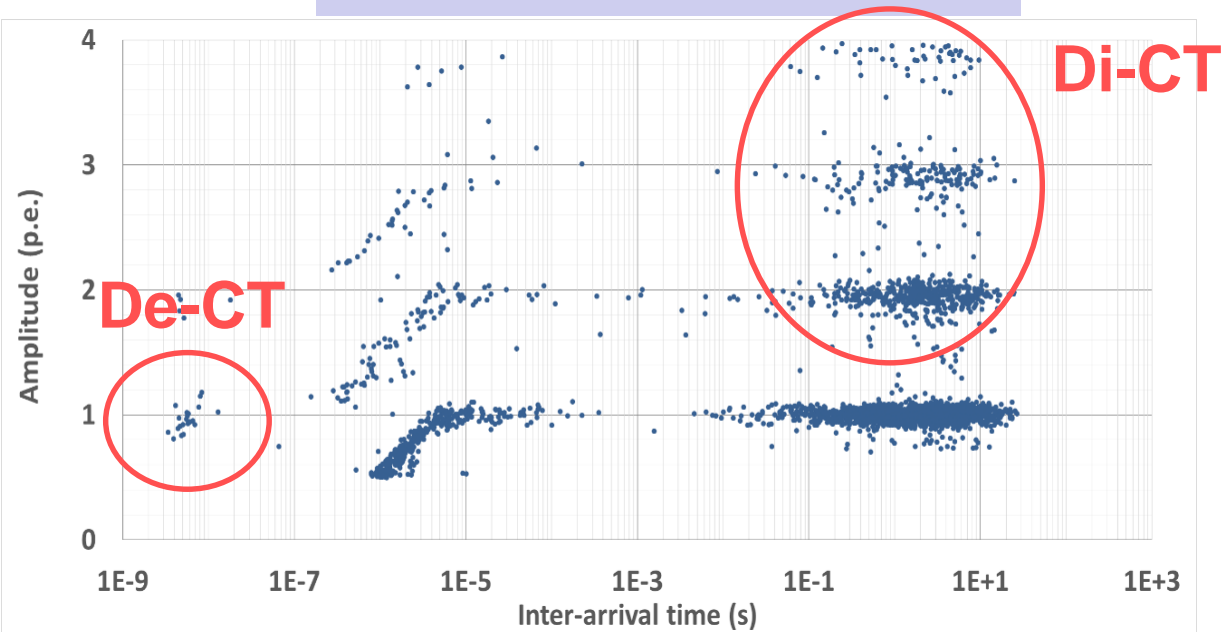
[A. Lacaita et al., IEEE TED, vol. 40, n. 3, 1993]

Optical cross-talk

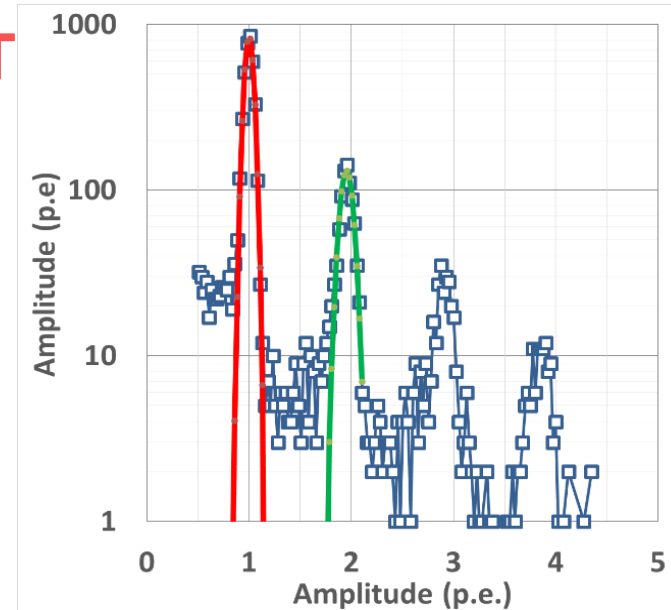


CT measurement

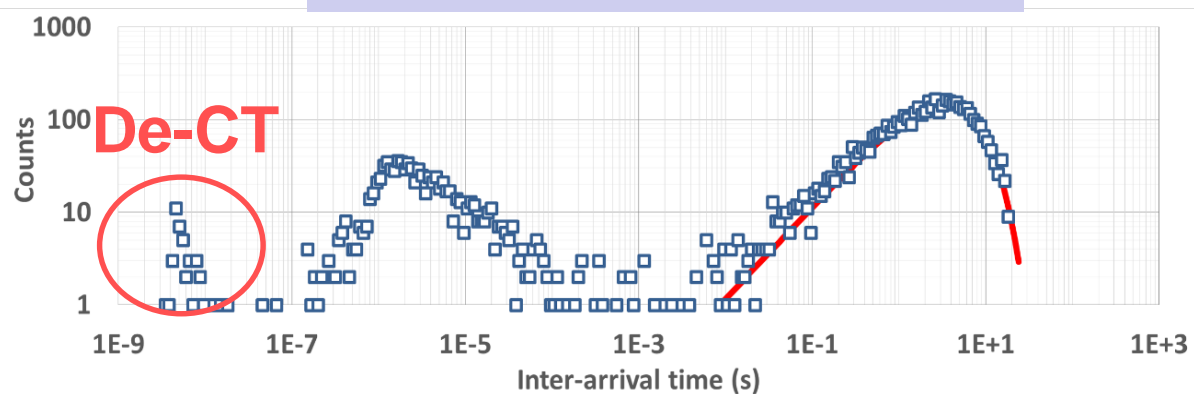
Scatter plot



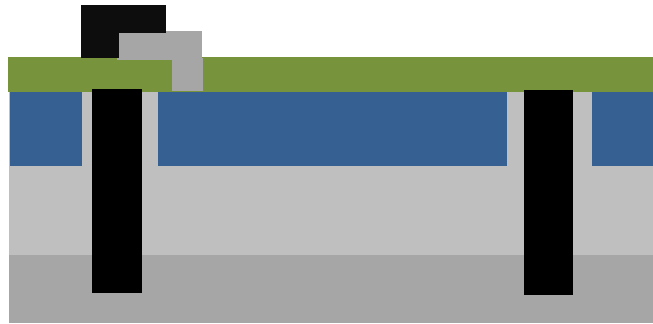
Amplitude histogram



Inter-arrival time histogram



CT in NUVV-HD



Direct cross-talk

Delayed events

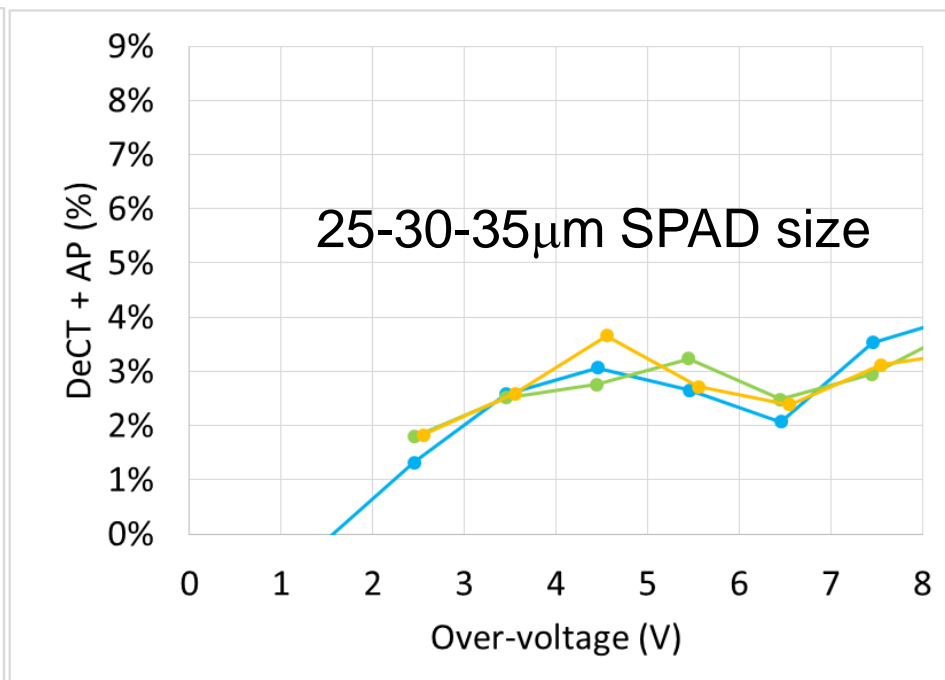
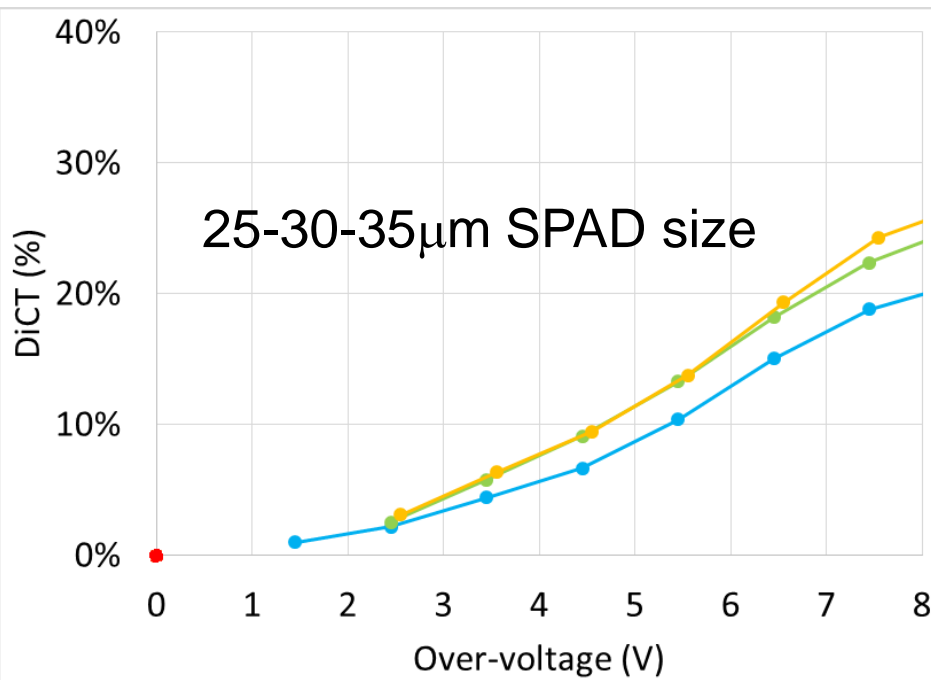


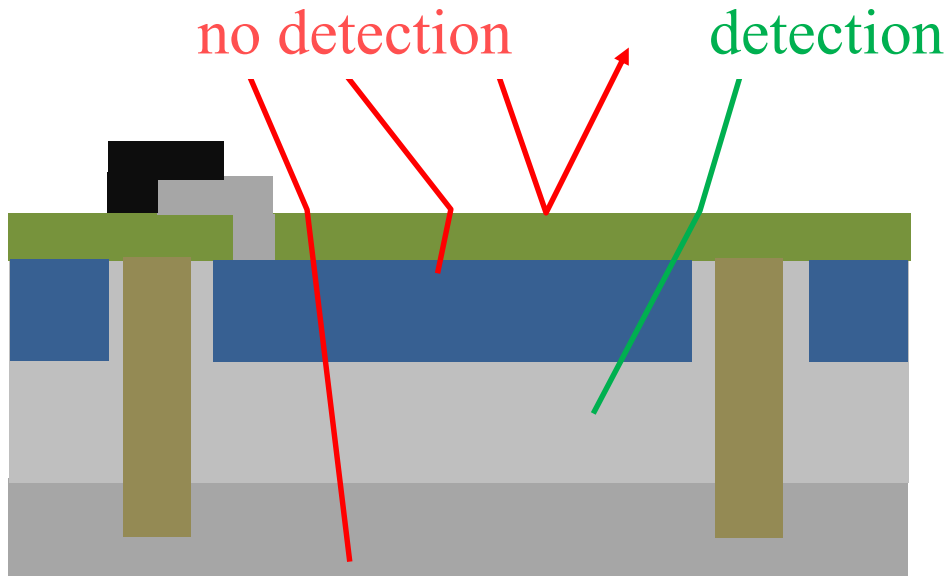
Photo-detection efficiency

$$\text{PDE}(V, \lambda) = \text{FF} \times \text{QE}(\lambda) \times T_P(V, \lambda)$$

SPAD
Fill Factor

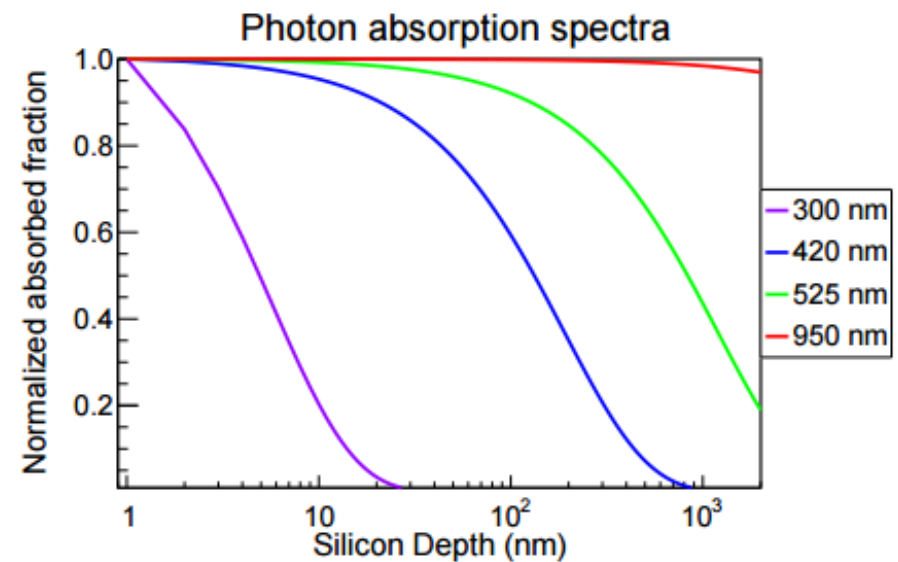
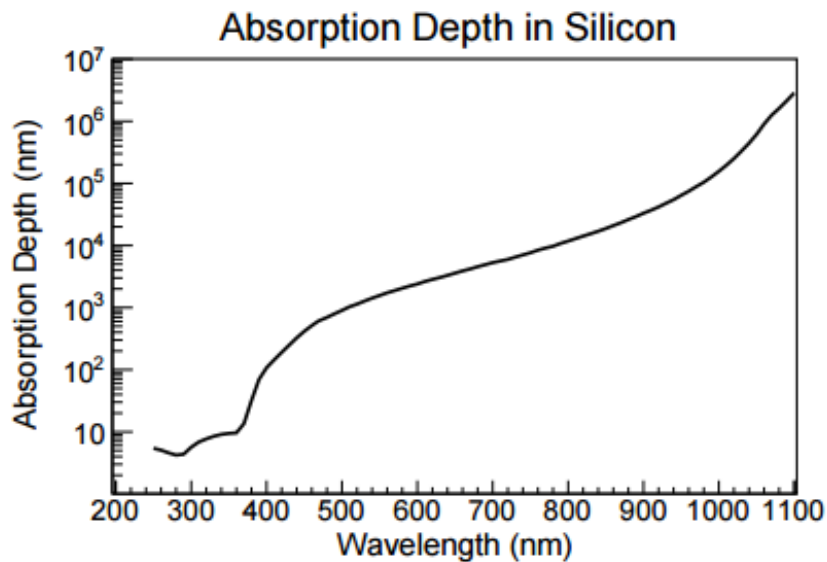
Quantum
Efficiency

Triggering
Probability



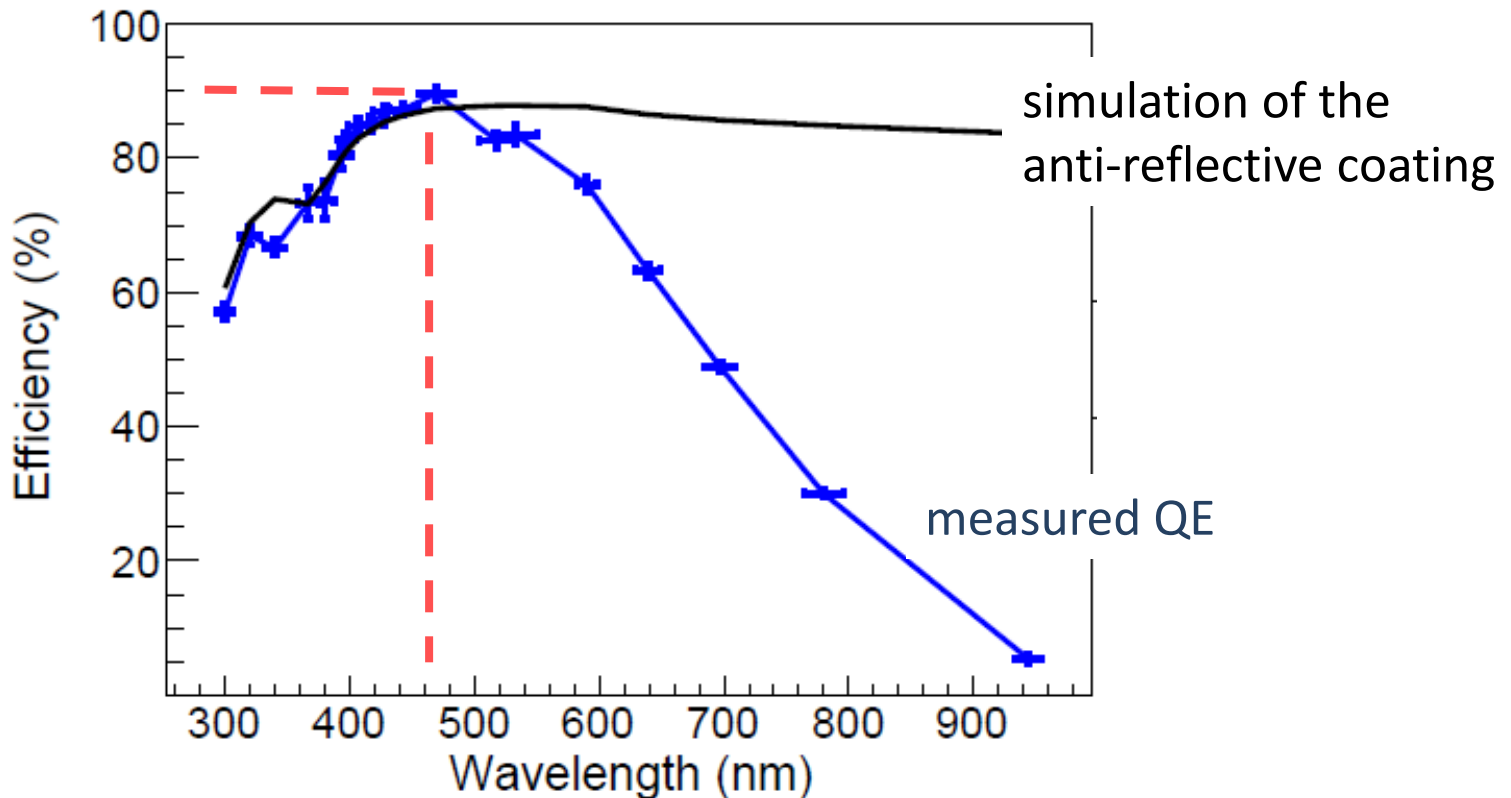
It depends on:

- Anti-reflective coating
- active layer thickness
- junction depth



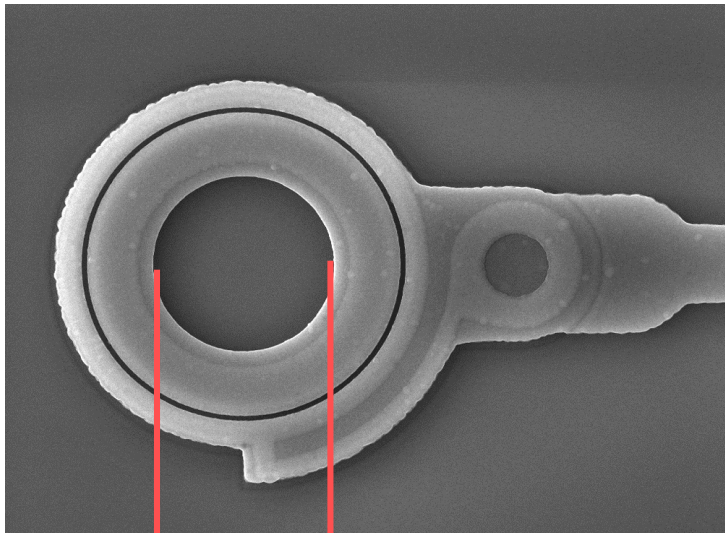
NUV-HD: QE

QE Measured on a photodiode produced with SiPMs
+
Simulation of the anti-reflective coating

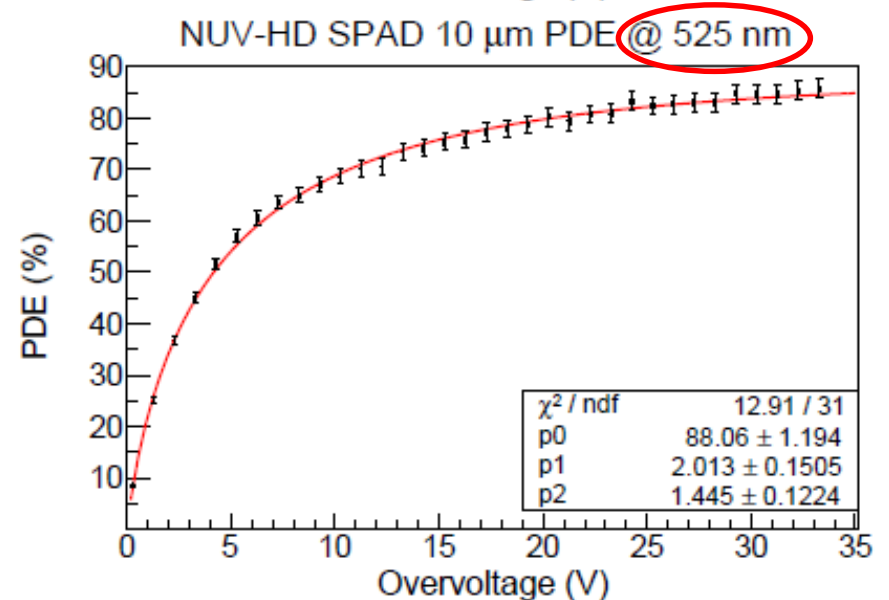
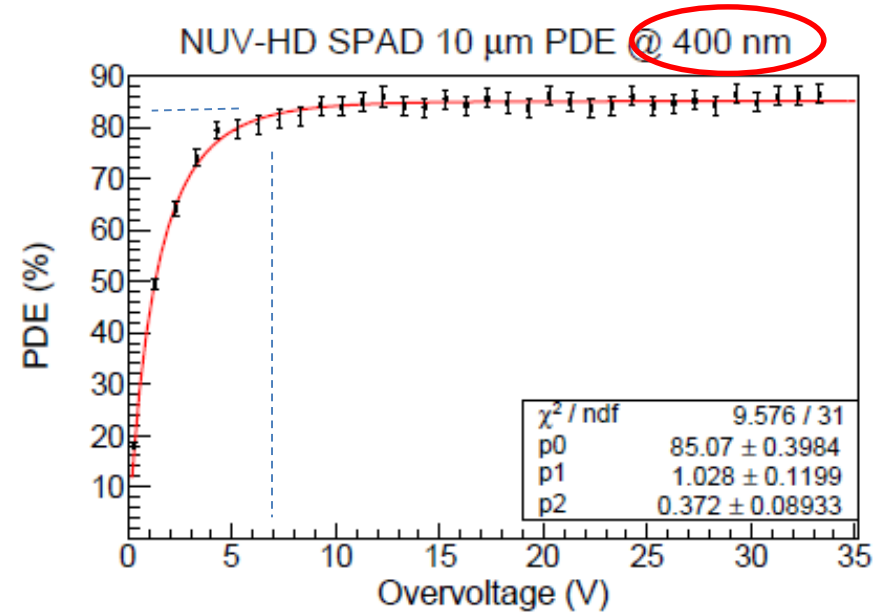


NUV-HD: QE*Pt

cSPAD (100% Fill Factor)

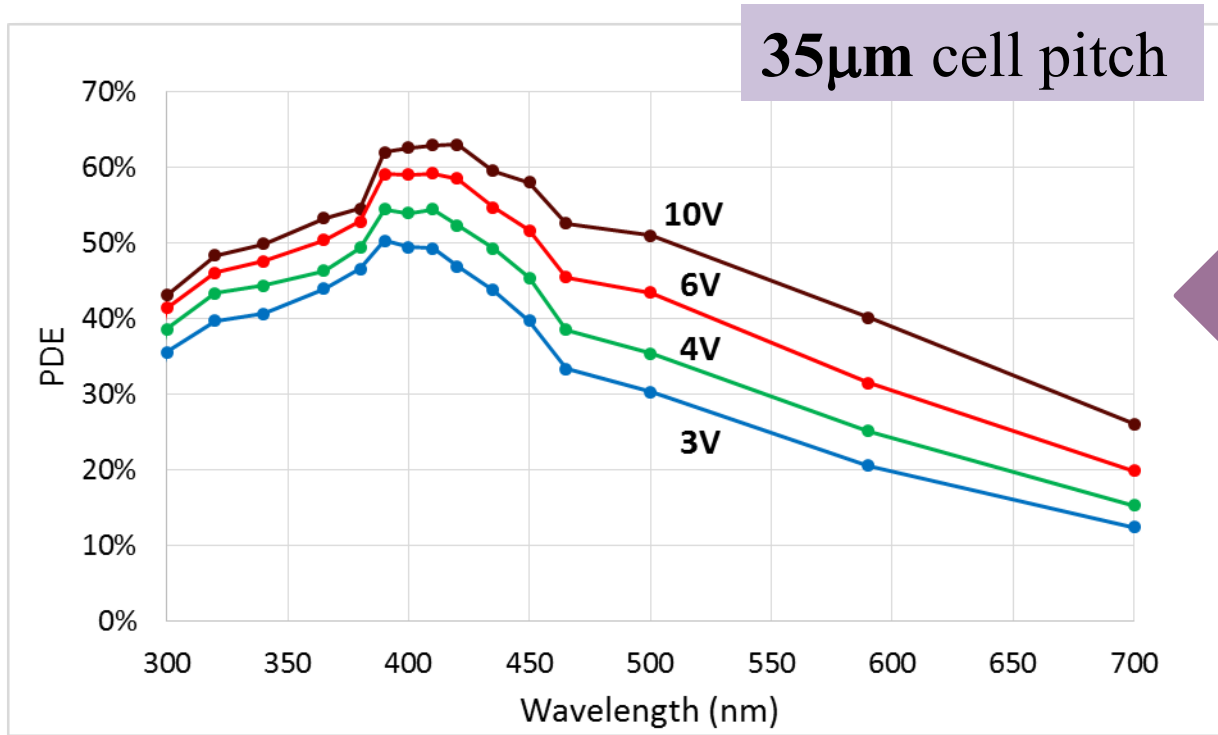


SPAD size is defined by metal opening which is within the high-field region



NUV-HD: PDE

SPAD Pitch	15 μm	20 μm	25 μm	30 μm	35 μm	40 μm
Fill Factor (%)	55	66	73	77	81	83
SPAD/mm ²	4444	2500	1600	1111	816	625



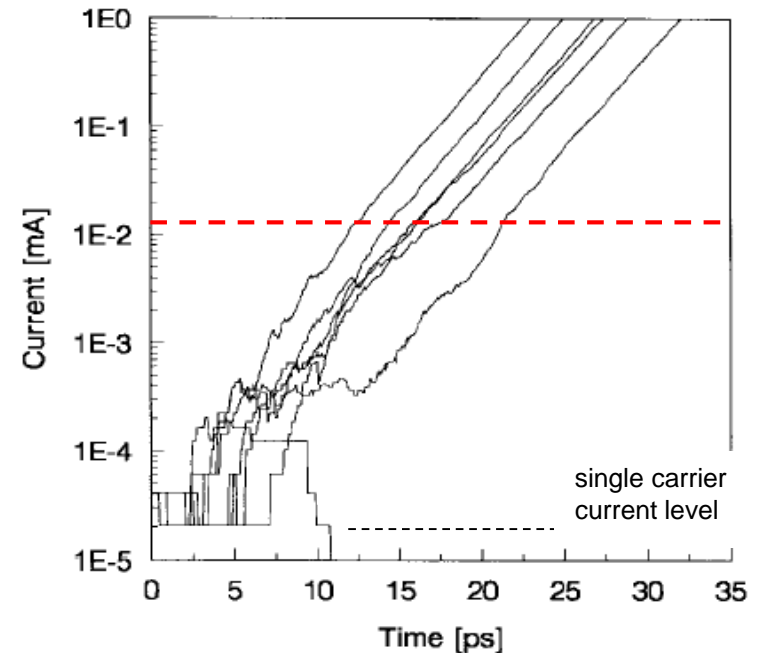
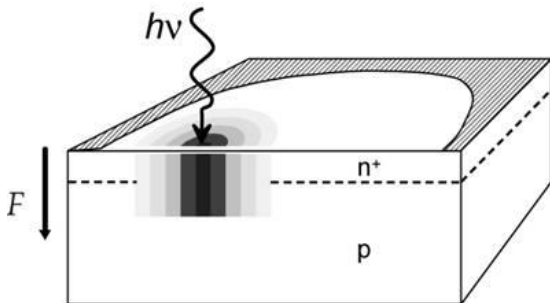
Intrinsic Time jitter

Statistical Fluctuations in the current growth:

1. **Photo-conversion depth**
2. **Vertical Build-up** at the very beginning of the avalanche

$t=0$ pair generation
 $0 < t < t_1$ drift to the high-field region
 $t > t_1$ avalanche multiplication

3. **Lateral Propagation**



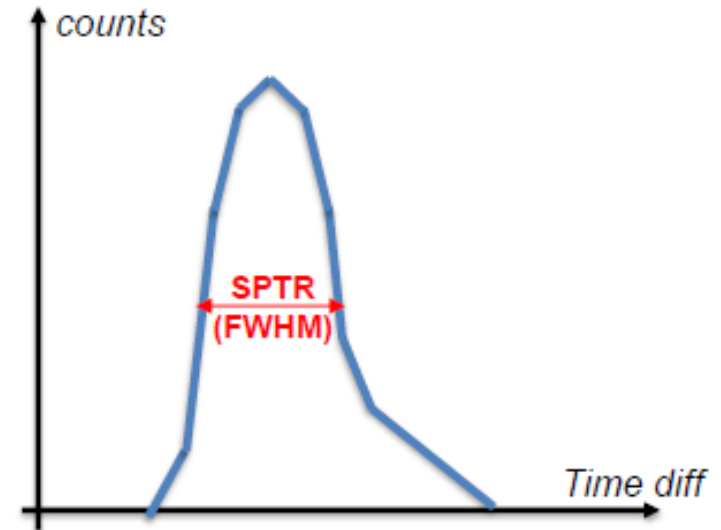
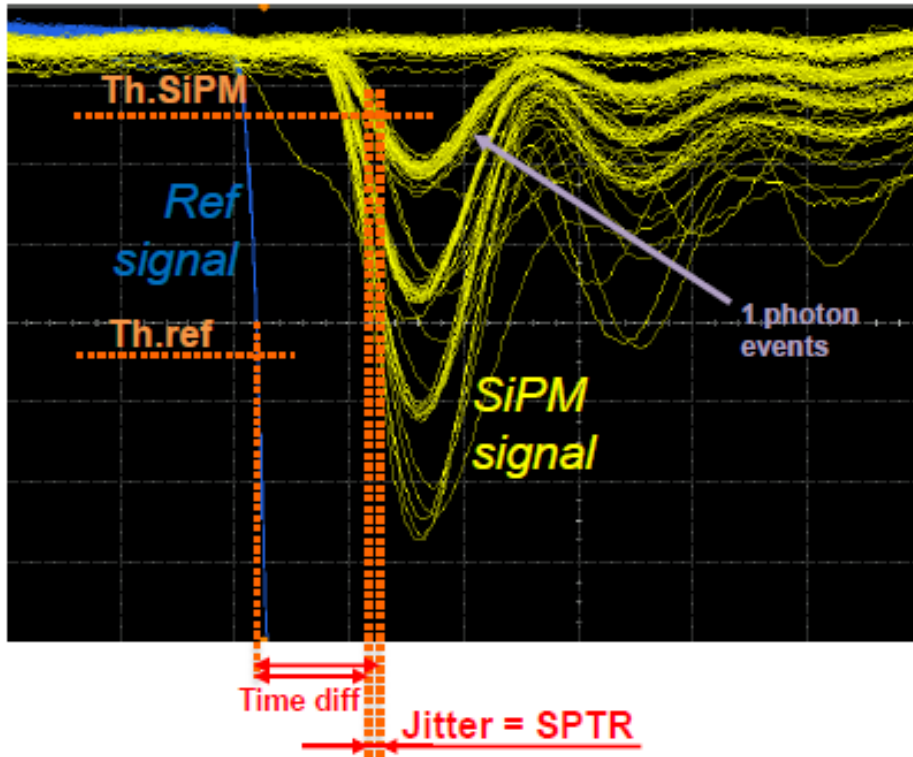
IEEE TRANSACTIONS ON ELECTRON DEVICES, VOL. 44, NO. 11, NOVEMBER 1997

1931

Physics and Numerical Simulation of Single Photon Avalanche Diodes

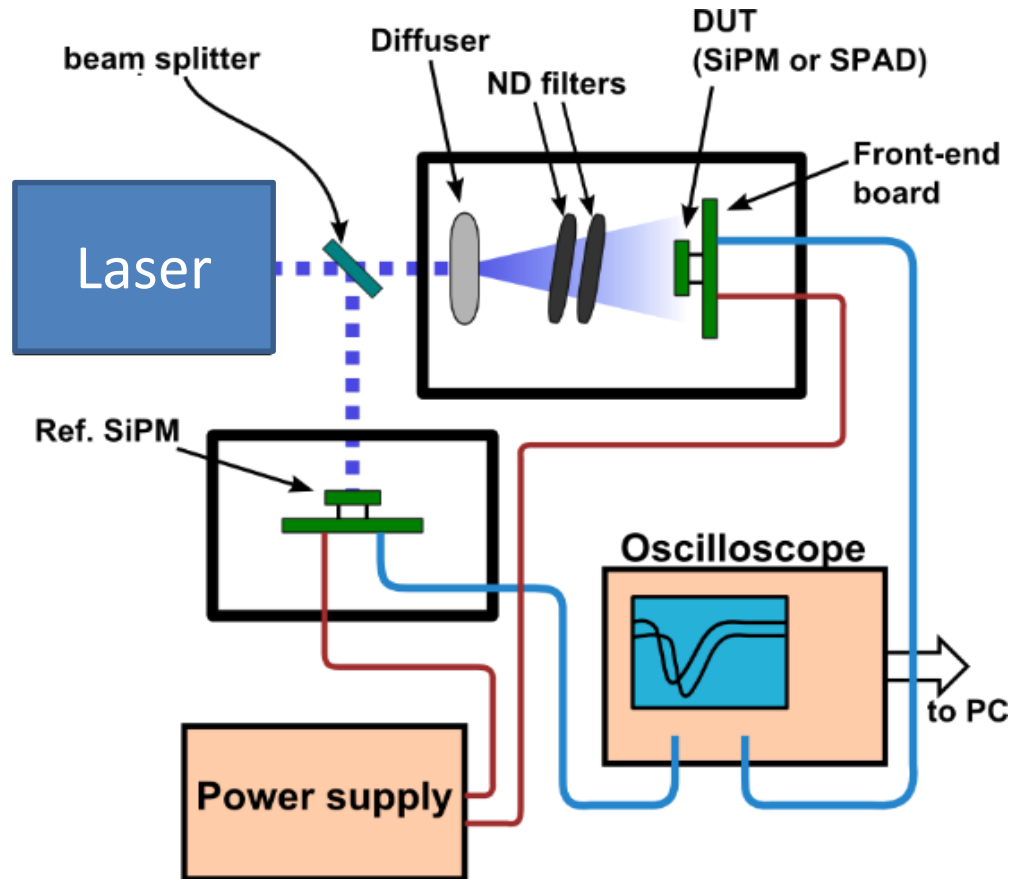
Alessandro Spinelli and Andrea L. Lacaita, *Senior Member, IEEE*

Single-photon time resolution (SPTR)



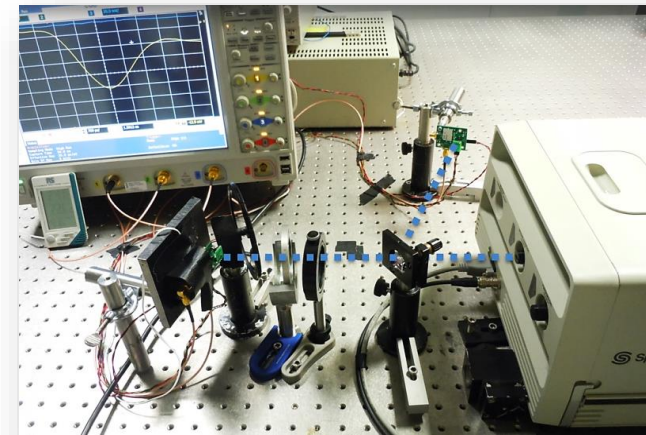
- **Single-photon time resolution: jitter in time between photon arrival on the SiPM and front end detection of the event**
- Typically measured FWHM

Measurement setup for SPTR

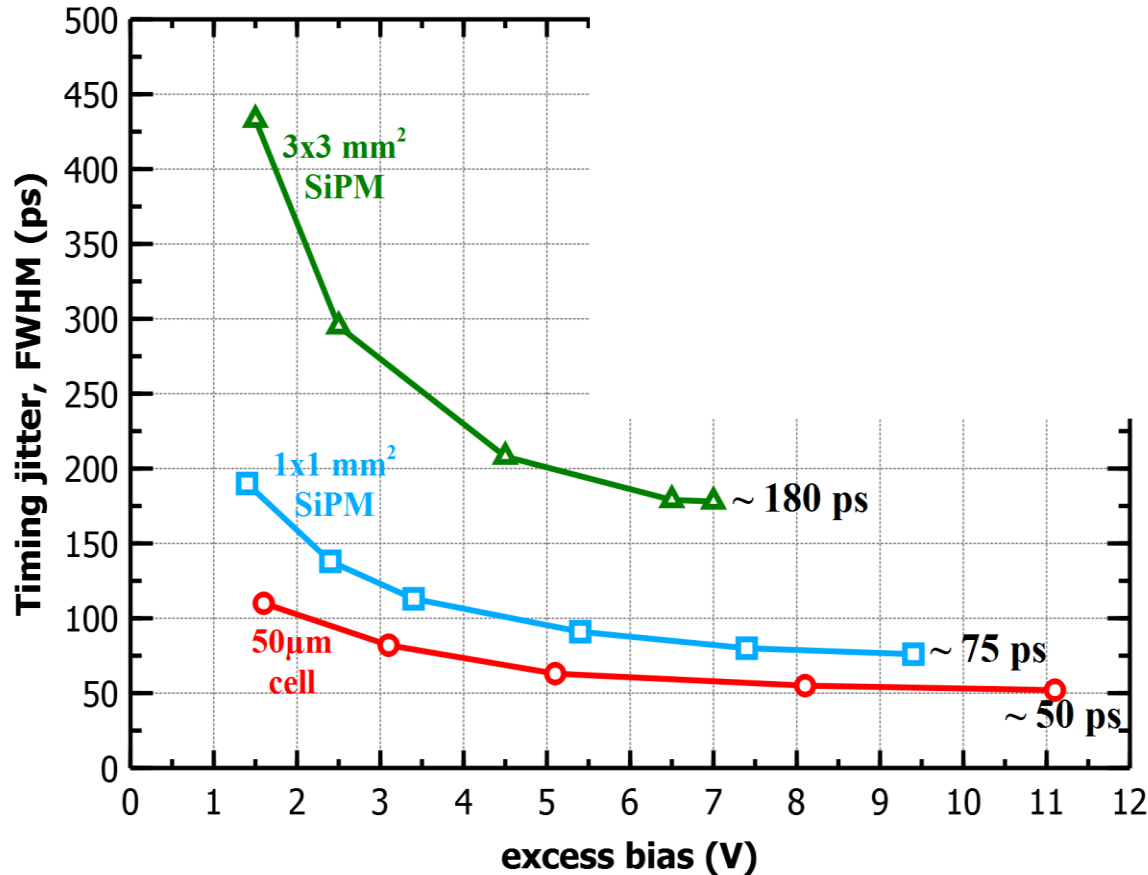


- 2-ps width pulsed laser (425nm)

- Set-up time resolution ~ 10 ps FWHM



Example of SPTR



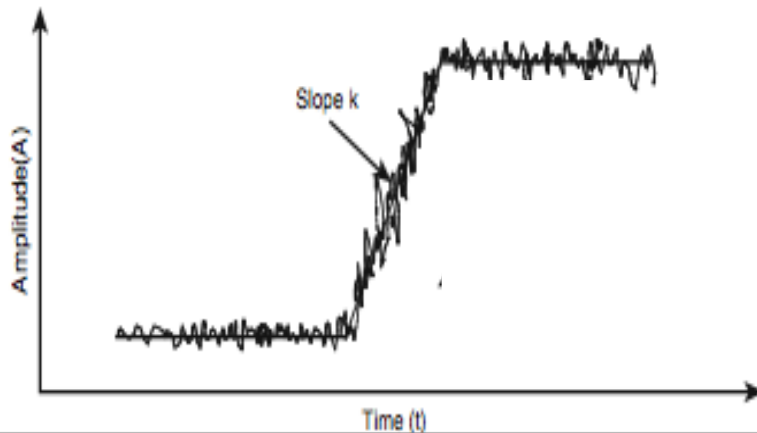
- SPAD (50x50µm²)
- 1x1mm² SiPM of 50x50µm²
- 3x3mm² SiPM of 50x50µm²

F. Acerbi, et al IEEE TNS vol. 61, n. 5, 2014 , pp. 2678 - 2686

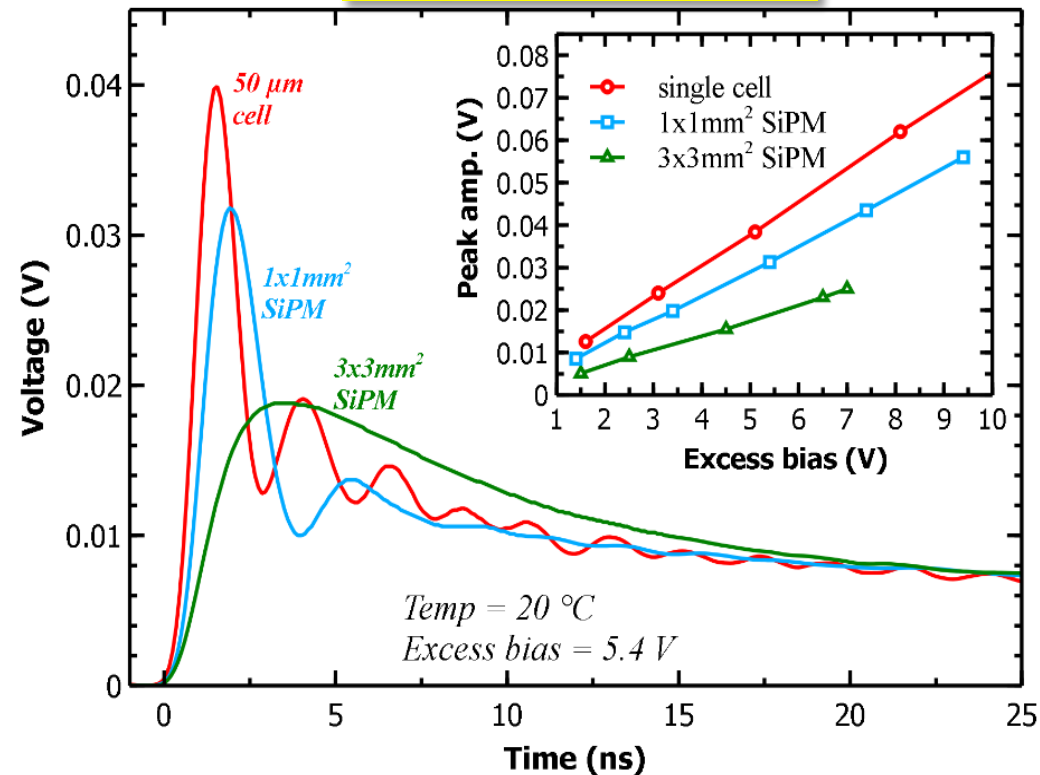
Noise contribution to SPTR

Is the electronic noise the origin of SPTR deterioration moving to large areas?

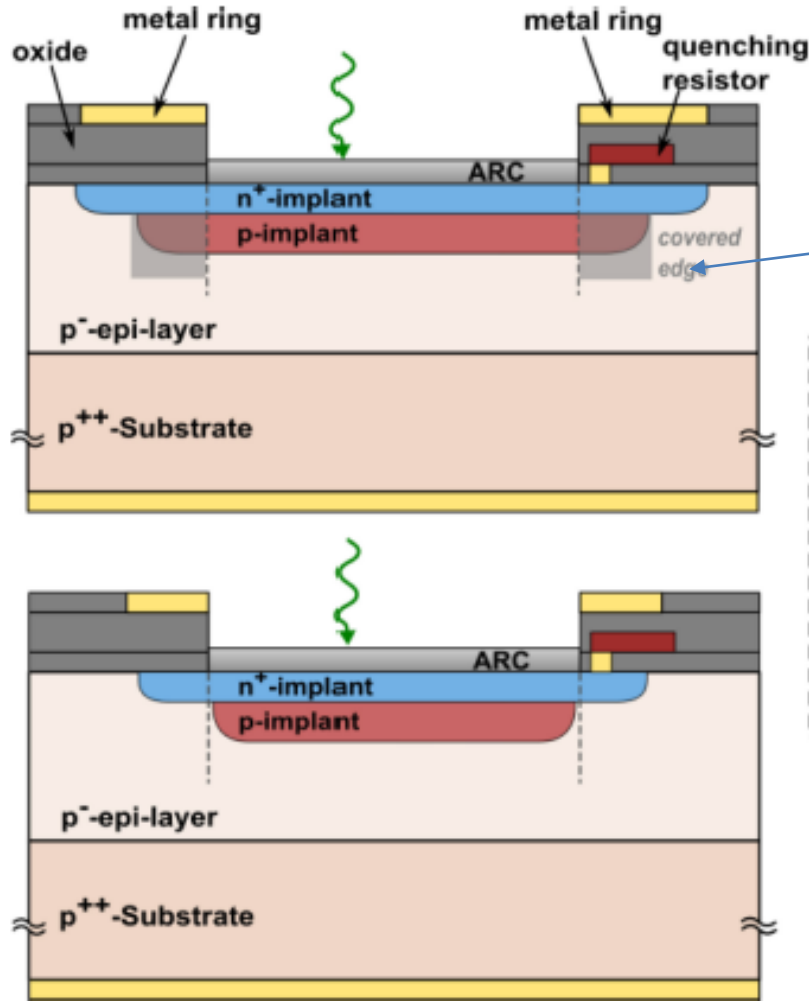
Signal shape



$$\sigma_t \propto \frac{\sigma_a}{f'_{th}}$$

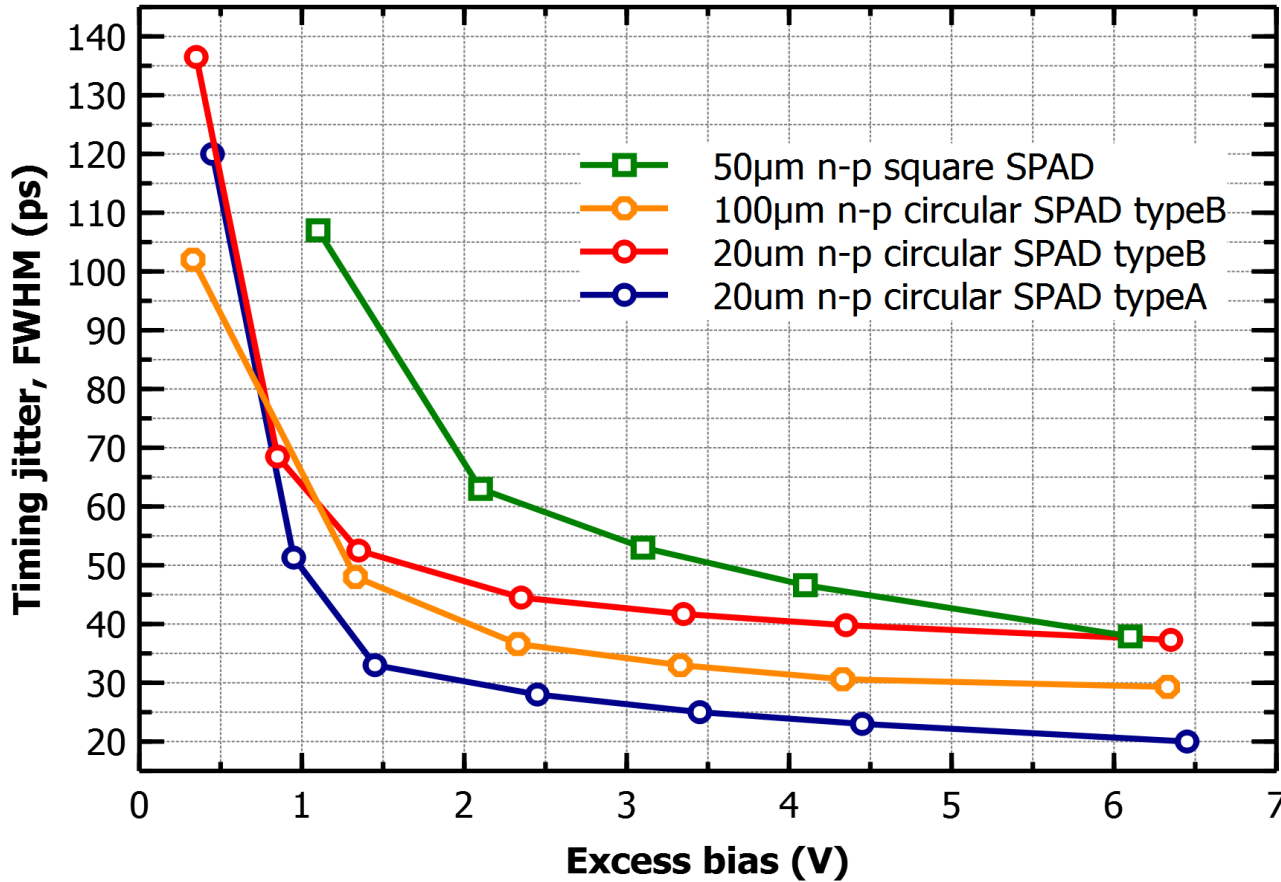


SPTR: ultimate limit?



We designed a small SPAD with masked edges.

SPTR: analysis at a single SPAD level



uncovered edge
 uncovered edge
 uncovered edge
 covered edge

20 ps FWHM!!!

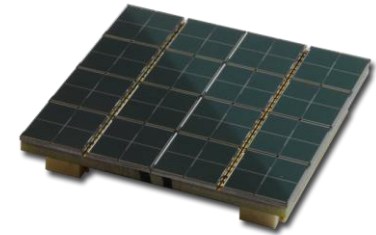
Metal ring all-around active area

- Better signal extraction
- more uniform signal shape

Main numbers in one table

Parameter	NUV-HD technology 1mm ² 40μm SPAD
DCR (20C)	<100 kHz
Di-CT	<20%
De-CT	<5%
AP (20C)	<5%
PDE	60% (400nm)
SPTR	80 ps FWHM

PMT vs SiPM for NUV light



}	compactness	↓	↑
	robustness	↓	↑
	sensitivity to magnetic fields	↓	↑
	low operating voltage	↓	↑
}	PDE	↑	↑
	DCR	↑	↓
	dynamic range	↑	↓
}	SPTR	↑	↑
	cost	↑	~↑
	market competition	↓	↑

Hot topics in SIPM/SPAD

- High Dynamic Range
- NIR sensitivity

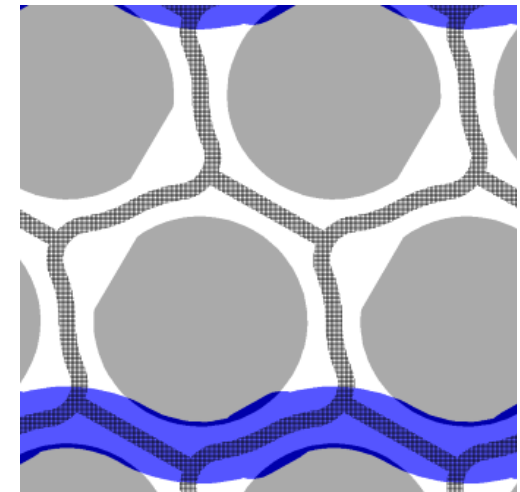
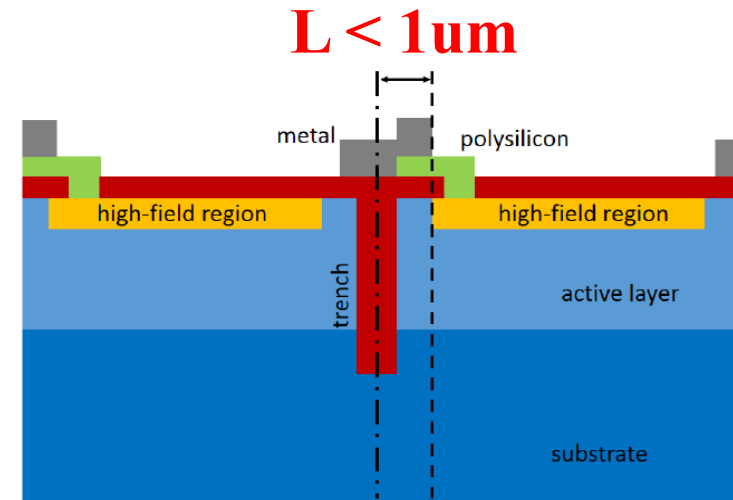
FBK is working on those aspects.
UHD technology is an example.

New design

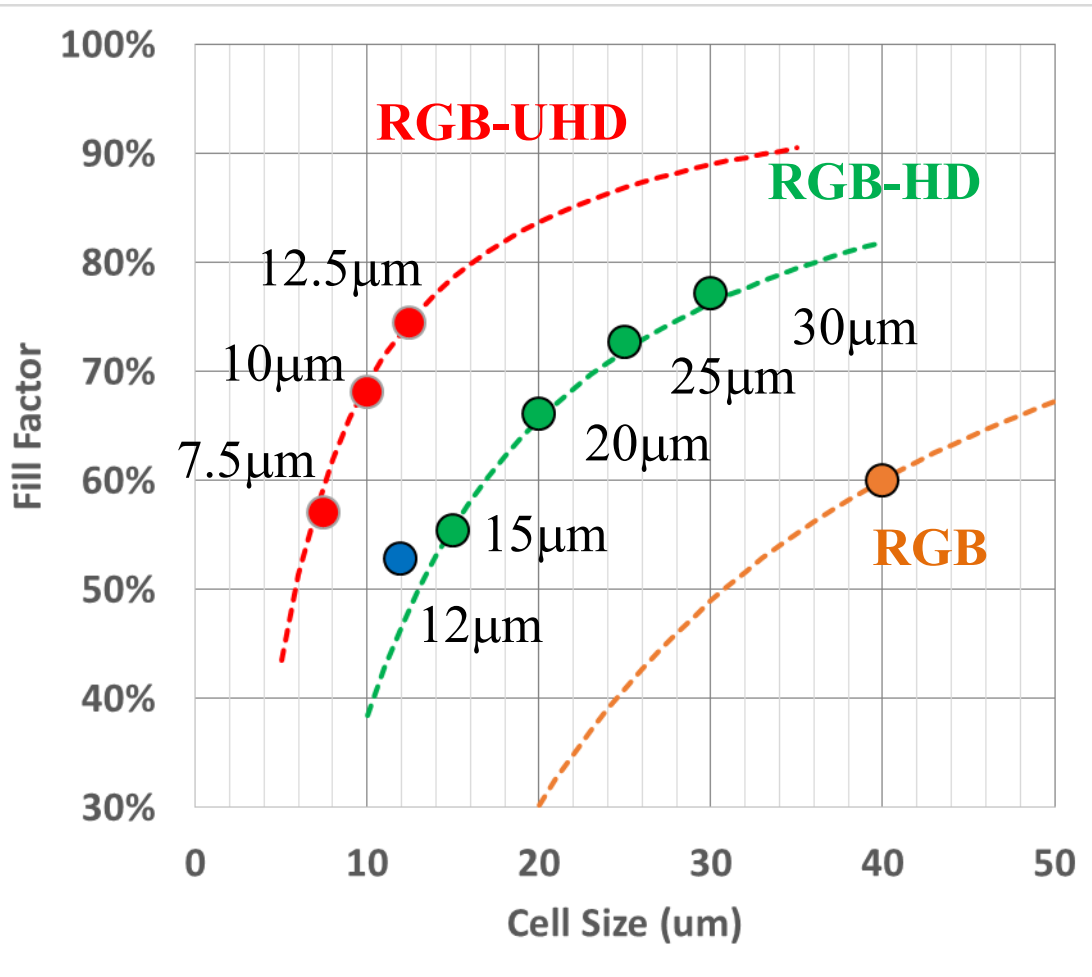
Reduction of all the feature sizes

Circular active area (smallest cells)

- No corners (with lower field)
- Hexagonal cells arranged in honeycomb configuration



HD technology: small cells



RGB-HD

cell pitch (µm)	cells/mm ²
12	7000
15	4500
20	2500
25	1600
30	1100

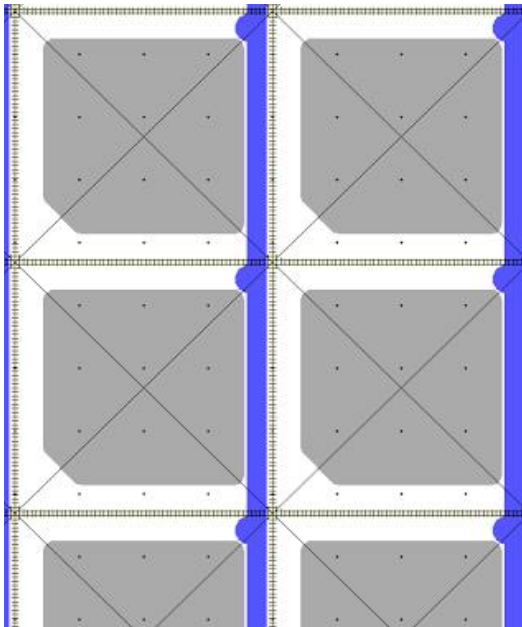


RGB-UHD

cell pitch (µm)	cells/mm ²
7.5	20530
10	11550
12	7400

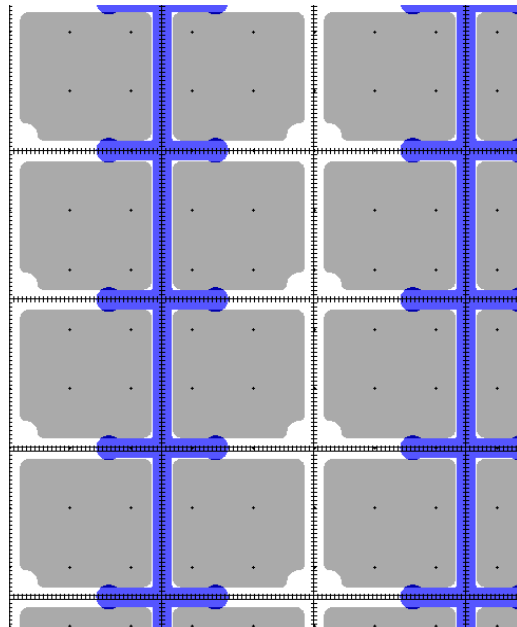
Comparison to other technologies

40 um cell



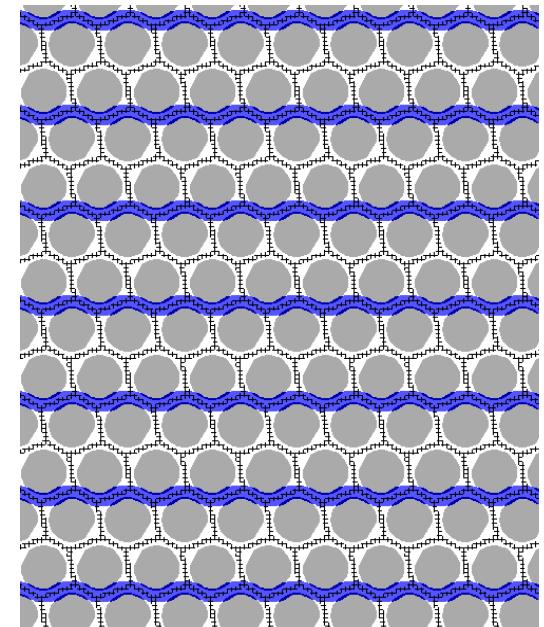
RGB
SiPMs

25 um cell



RGB-HD
SiPMs

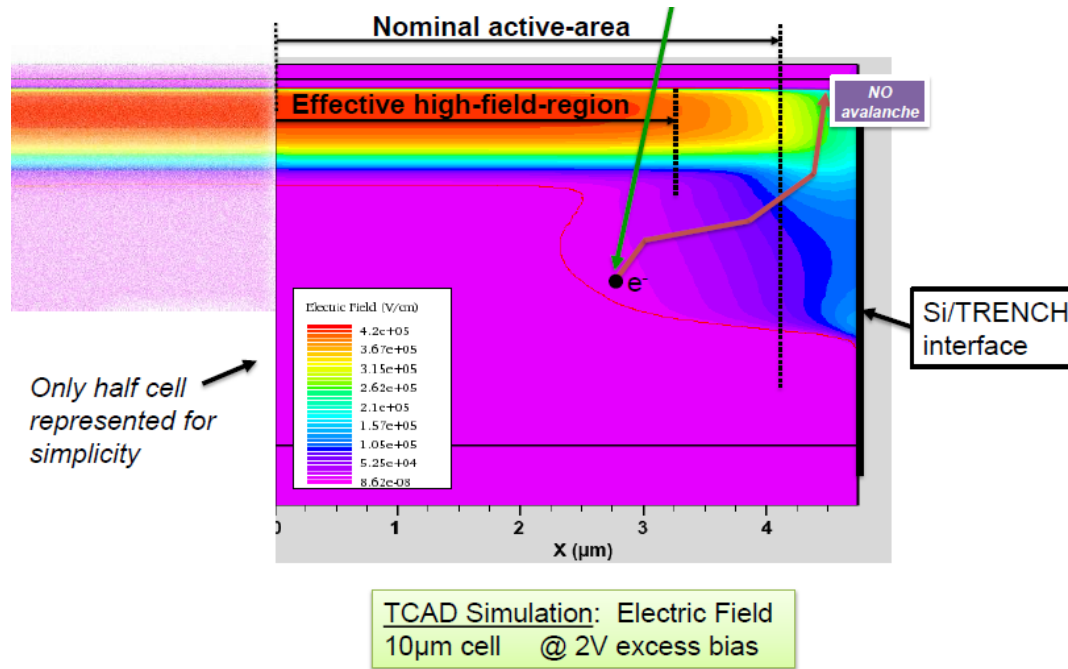
<7.5 um cell



RGB-UHD
SiPMs

...new design is not enough...

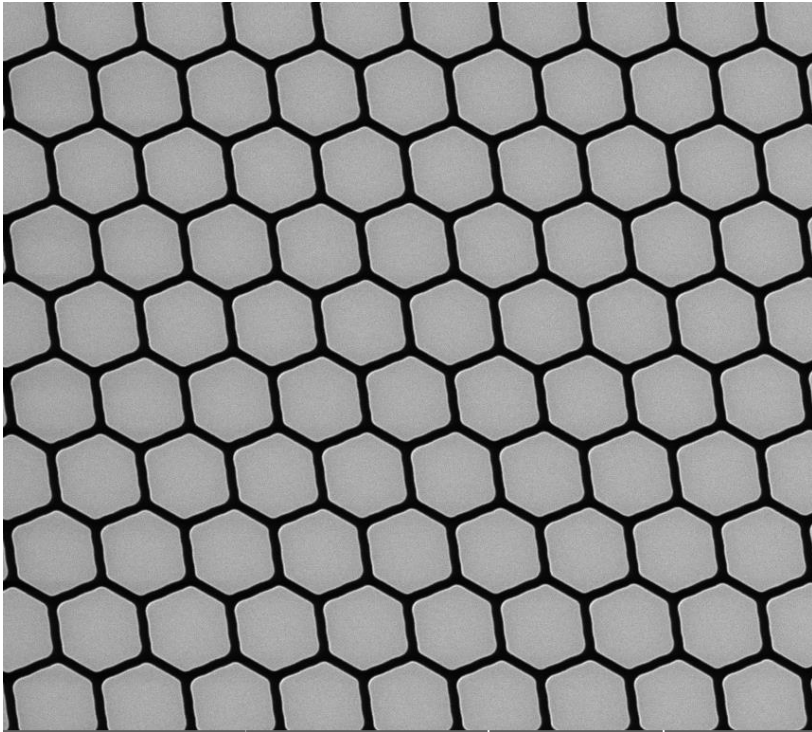
Border region plays an important role for small cells.



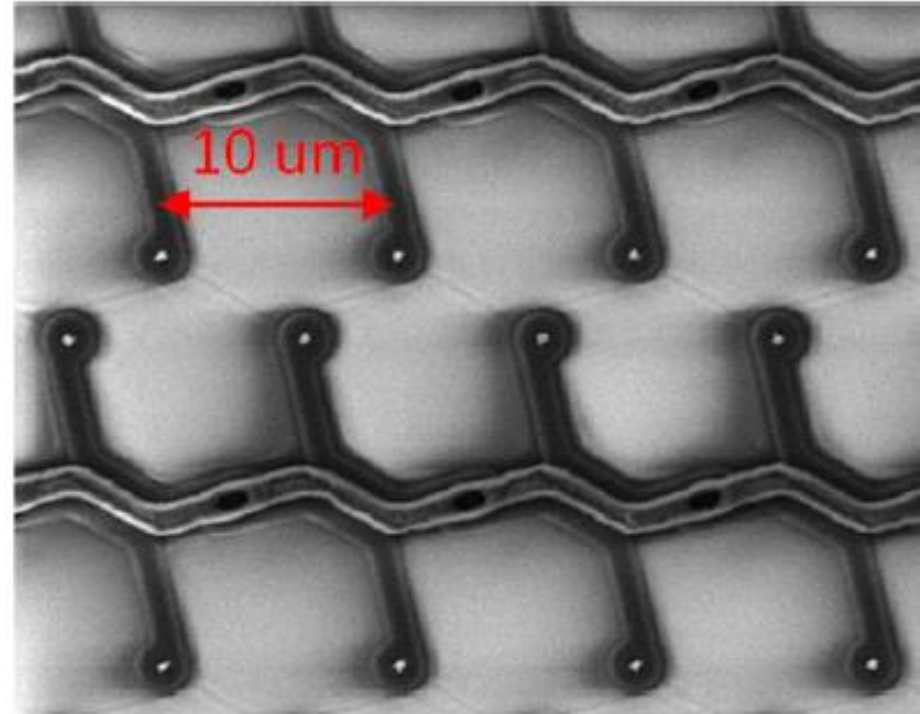
We have to develop a new guard ring (NGR) especially for the smallest SPAD (5µm)

F.Acerbi et al., presented at IEEE NSS, Strasbourg 2016

SEM images



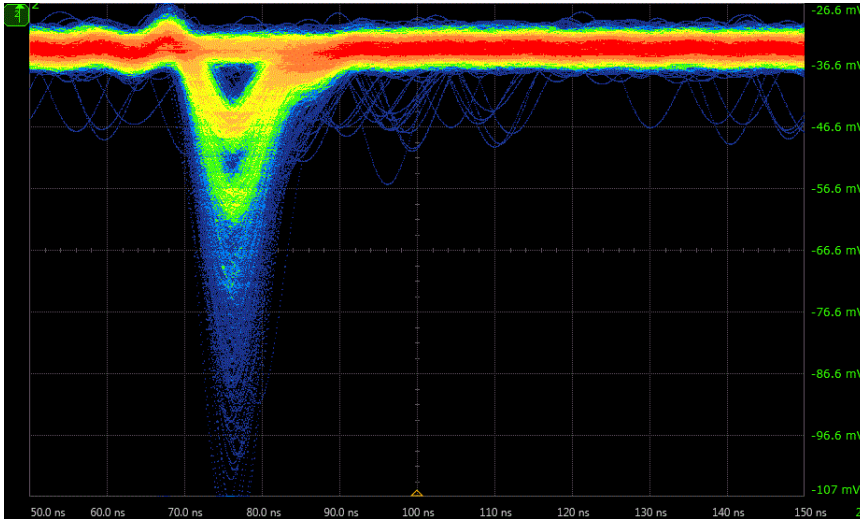
Microcells separated by trenches (picture taken during processing)



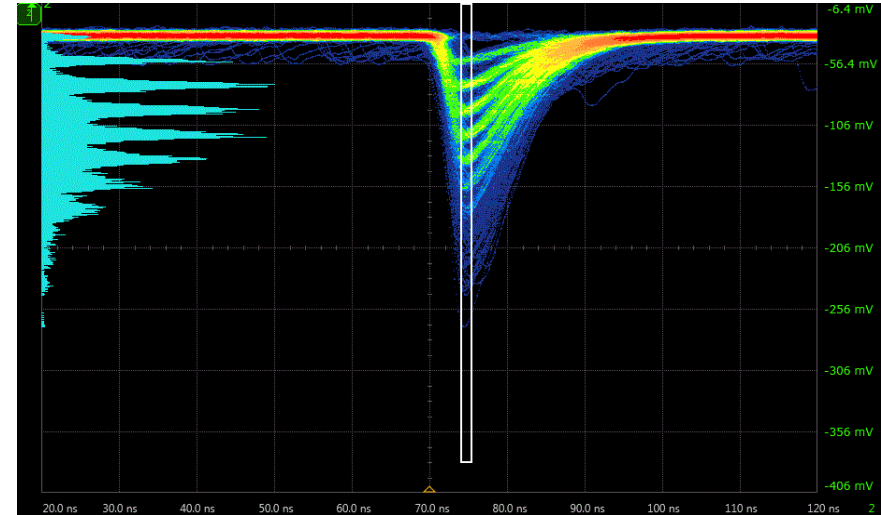
Finished SiPM
(10 um)

Oscilloscope waveforms

7.5 um cell



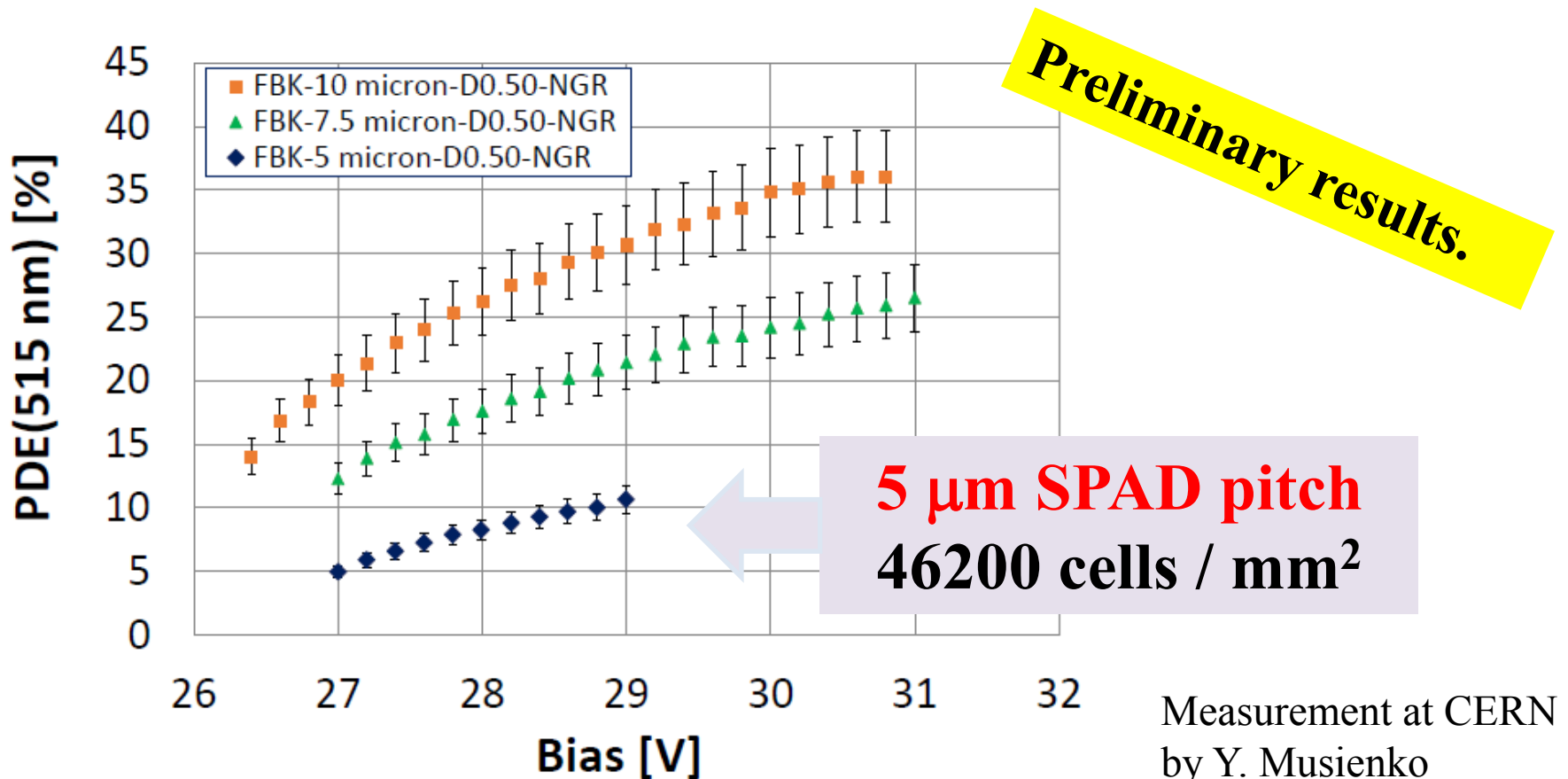
10 um cell



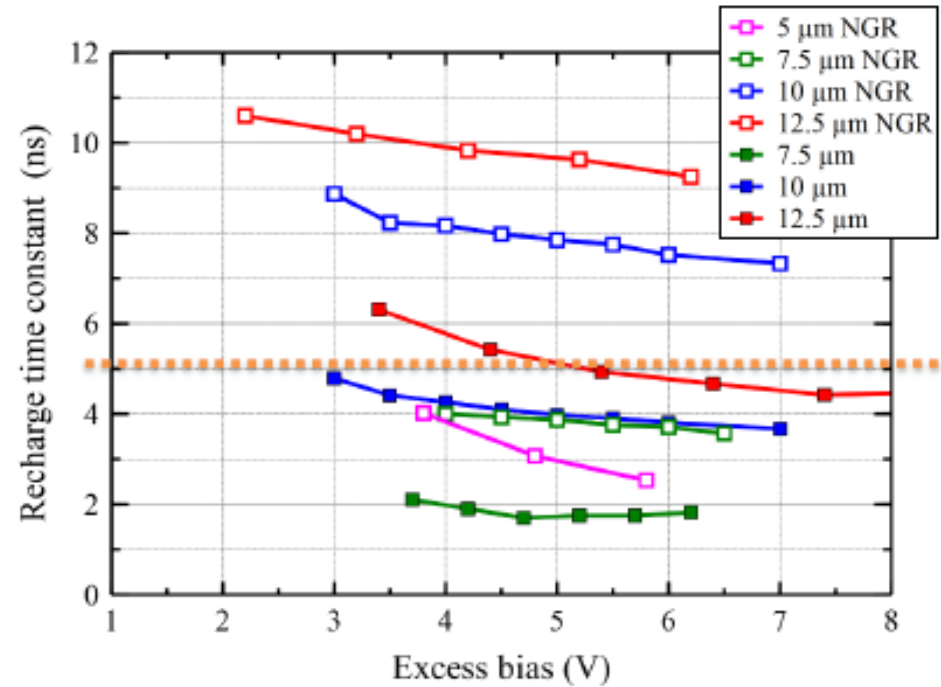
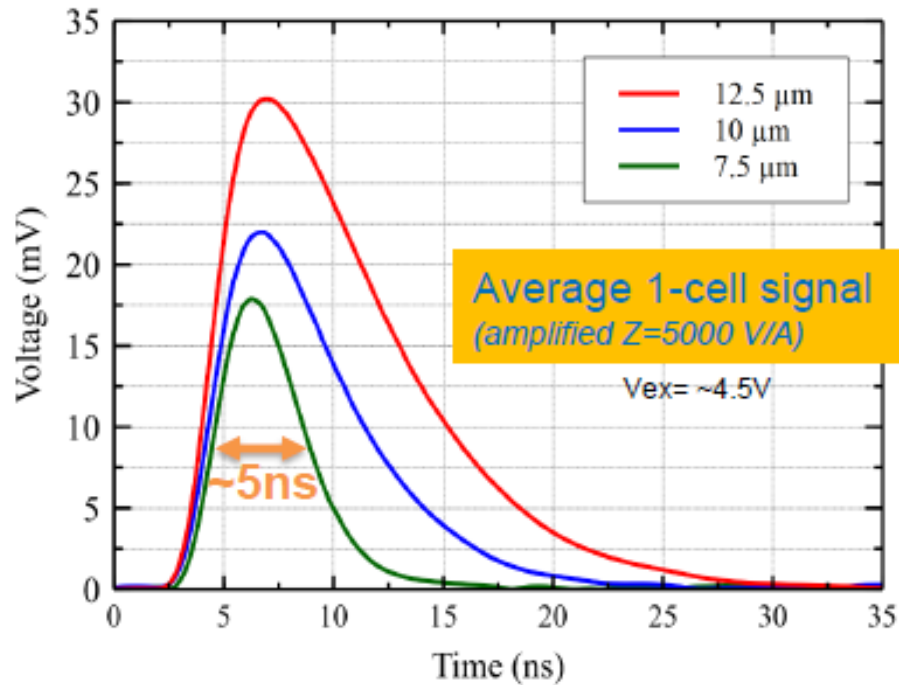
The 5um SPAD does not work with the standard guard ring while **it works with NGR!!**

RGB-UHD: PDE

- Optimization of the technology
- Development of even smaller cell size



RGB-UHD: Signal



Thanks to all collaborators

Fabio Acerbi
Giacomo Borghi
Gabriele Faes
Nicola Furlan
Alberto Gola
Marco Marcante
Stefano Merzi
Claudio Piemonte
Giovanni Paternoster
Antonino Picciotto
Veronica Regazzoni
Nicola Zorzi

